Manawatū Gorge Landslide Dam Hazard Assessment

S Dellow
S de Vilder
R Morgenstern
P Upton

GNS Science Consultancy Report 2019/103
October 2019

DISCLAIMER

This report has been prepared by the Institute of Geological and Nuclear Sciences Limited (GNS Science) exclusively for and under contract to Horizons Regional Council. Unless otherwise agreed in writing by GNS Science, GNS Science accepts no responsibility for any use of or reliance on any contents of this report by any person other than Horizons Regional Council and shall not be liable to any person other than Horizons Regional Council, on any ground, for any loss, damage or expense arising from such use or reliance.

Use of Data:

Date that GNS Science can use associated data: July 2019

BIBLIOGRAPHIC REFERENCE

Dellow S, de Vilder S, Morgenstern R, Upton P. 2019. Manawatū Gorge landslide dam assessment. Lower Hutt (NZ): GNS Science. 52 p. Consultancy Report 2019/103.

CONTENTS

FIGURES

TABLES

APPENDICES

EXECUTIVE SUMMARY

The slopes of the Manawatū Gorge are susceptible to large landslides that could dam the Manawatū River. Such landslide dams result in upstream flooding, as a lake forms behind the dam, and downstream flooding in the event of the dam failing. The potential impacts of a large landslide damming the Manawatū Gorge and the associated flooding impacts have been assessed by: determining largest credible landslide in the gorge, identifying locations where such a landslide could occur, calculating dam heights from the landslide runout, and modelling the extent of upstream flooding by the formation of a lake and the extent of downstream flooding in the event of dam failure.

Empirical evidence from greywacke slopes in similar terrain indicates that the largest credible landslide likely to form in the gorge has an area of 27,000 m^2 and volume (based on area to volume scaling relationships) of 118,000 m^3. These values are consistent with the largest historical landslide in the gorge.

Topographic stress modelling of the Manawatū Gorge indicates that the most susceptible slopes to failure are also in broad agreement with the historical record of landslides, and 10 of these sites were chosen for further analysis. Runout modelling at all 10 sites indicates a consistent minimum dam height of 10 m regardless of its location (upper, middle, lower) within the gorge. These landslides have then been used to establish the minimum height of a landslide dam and to determine the maximum extent of upstream flooding and the volume of water available to contribute to a debris flood downstream should the dam fail rapidly.

The location of the dam within the gorge determines the extent of flooding both upstream and downstream. At a dam crest height of 10 m, upstream flooding will not reach Woodville from the most upstream of the 10 modelled dams. Downstream flooding from rapid failure of the modelled dams may reach the low river terrace below Ashhurst. Despite this, the township is unlikely to be affected, as Ashhurst is built on a higher terrace and is protected from flooding in the Pohangina and the Manawatū Rivers. Flooding is unlikely to affect Palmerston North beyond the confines of flood protection adjacent to the Manawatū River.

The longevity of a landslide dam forming in the Manawatū Gorge was assessed using the Dimensionless Breach Index (DBI). This method indicates that a landslide dam forming in the Manawatū Gorge has a 90% chance of failing. Based on the behaviour of a similar landslide dam on the Clarence River, which failed 16 hours after the Kaikōura Earthquake, it is anticipated that a landslide dam in the Manawatū Gorge should be similarly short-lived.

It is recognised that the landslide modelling software does not accurately replicate the distinct cone shape deposits typically produced by large landslides in greywacke terrain. Research is currently being conducted to improve this and more accurate runout models could be produced in the future if required.

This page left intentionally blank.

1.0 INTRODUCTION

1.1 Background

The Manawatū River flows from the eastern side of the main axial ranges of the North Island through the Manawatū Gorge to the west coast near Foxton. In the Manawatū Gorge, the river has deeply incised a 6 km long ravine through greywacke, separating the Tararua Ranges in the south from the Ruahine Ranges in the north. The Manawatū River flows through the gorge at an elevation of 50–60 metres above sea level (m a.s.l.), with the crest of the slopes through the gorge at elevations ranging from 200–360 m a.s.l. The active faults that characterise the North Island Dextral Fault Belt in the area lie immediately to the east of the gorge (Ruahine and Mohaka Faults), resulting in a high seismic hazard for the study area.

Natural dams created by large landslides are common in New Zealand. The 2016 Kaikōura Earthquake resulted in the formation of nearly 200 landslide dams in the north-eastern South Island. Some of these dams eventually failed rapidly; however, the results were not catastrophic because the possibility for rapid failure of these dams was recognised and the potential consequences mitigated. Other examples of landslide dams that have failed rapidly in New Zealand include the 1998 rock avalanche dam in the Poerua River in South Westland (Hancox et al. 1999) and a landslide dam in the Mōkihinui Gorge caused by the 1929 Murchison Earthquake.

The potential for a landslide dam in the Manawatū Gorge and the consequences of it failing rapidly may represent a significant hazard to parts of the Horizons region. Consequently, Horizons District Council have commissioned GNS Science (GNS) to assess the potential of a large landslide blocking the Manawatū River and the possible flooding consequences both upstream of the dam and downstream in the event of a rapid dam failure. The flood hazards are assessed to enable appropriate risk management and mitigation strategies to be developed by Horizons Regional Council.

1.2 Objectives and Methods

The main objective of this project is to estimate the maximum credible landslide volume that could potentially dam the Manawatū River, evaluate the potential landslide source areas in the Manawatū Gorge where such landslides could initiate from and evaluate the flooding impacts both upstream of the dam and downstream should a catastrophic dam failure occur.

To achieve this objective, the following steps were taken:

1. Empirical analysis of greywacke landslides caused by the 2016 Kaikōura Earthquake. Landslide size distribution on slopes similar to those in the Manawatū Gorge were investigated to identify the largest landslides that occurred in the 2016 Kaikōura Earthquake on similar (height and slope gradient) greywacke slopes.
2. Empirical analysis of the size distribution of previous mapped greywacke landslides in the Manawatū Gorge.
3. Development of 38 cross-sections through the Manawatū Gorge to characterise its topography.
4. Analysis of these cross-sections to determine the sites most susceptible to failure from slope angle / slope height relationships.

5. Quantification of the largest credible landslide that could form within the Manawatū Gorge determined from empirical data, which was used to inform the numerical modelling.
6. Numerical modelling of landslides for 10 cross-sections with failure modes assumed to be controlled by rock mass strength properties.
7. Determination of the minimum crest height of a landslide dam formed by the maximum credible landslide for at least five locations within the Manawatū Gorge, used for modelling upstream (inundation) and downstream (debris flood) effects.
8. Numerical modelling of debris flood outflow route from the maximum credible landslide dam at three sites through the Manawatū Gorge to determine flood heights downstream of the landslide dams.
9. Modelling of upstream inundation (maximum upstream flood level), with the reference level being the lowest point on the crest of the maximum credible landslide dam at each site.

The following data have been used to undertake the assessment described in this report:

1. Topographic data: Light Detection and Ranging (LiDAR) data from GNS files, Land Information New Zealand and Horizons Regional Council. For any area where LiDAR data were not available, the default dataset was the Topo50 20 m contour dataset.
2. Greywacke slope performance data, including:
    a. Slope height / slope angle curves for Wellington and Manawatū greywacke (Hancox et al. 2015),
    b. Empirical data on landslides in the Manawatū Gorge (from GNS files), and
    c. Landslide data from greywacke slopes that failed during the 2016 Kaikōura Earthquake (GNS files).
3. Greywacke rock mass properties from the characterisation of greywacke slopes in Wellington from the Ministry of Business, Innovation and Employment (MBIE) funded Endeavour Smart Ideas fund researching Anthropogenic Slope Hazards (Brideau and Massey 2019).

2.0 DATA SOURCES

2.1 LiDAR

All available 1 m LiDAR data were compiled within an area that spans 1–2 km either side of the Manawatū River throughout the gorge. Available LiDAR datasets were supplied by Horizons Regional Council and included: the Palmerston North City Council 2018 survey of Palmerston North City, the New Zealand Transport Agency (NZTA) 2013 Manawatū Gorge south survey, the New Zealand Transport Agency 2018 Manawatū Gorge north survey, the Horizons Regional Council 2016 LiDAR survey and the Horizons Regional Council 2005 and 2009 floodplain surveys.

Where possible, the most recent dataset was used; these were compiled in multiple stages. First, each of the various datasets was differenced from each of the neighbouring datasets in the study area and any disparities along the margins were removed. This was particularly the case in areas where engineering works have taken place along the state highway between the time periods of LiDAR capture. The datasets were then converted to point features and combined into a single seamless grid.

2.2 Landslide Inventories

The landslide inventory for the south side of the Manawatū Gorge, compiled and outlined in Hancox et al. (2013), was used to identify the largest landslide in the historical record within the gorge. Figure 2.1 displays the mapped distribution of landslides on the south side of the gorge from Hancox et al. (2013). The landslide with the largest area (and volume) in the inventory is a 2011 landslide. This landslide is the largest polygon on Figure 2.1 and has a source area of c. 27,000 m^2.

The comprehensive dataset of co-seismic landslides associated with the 2016 Kaikōura Earthquake (Massey et al. 2018) was analysed to constrain the largest credible landslide likely to occur in the Manawatū Gorge. Comparison between the two areas was justified because the geology and topography of coastal slopes in Kaikōura are similar to the ravine slopes in the Manawatū Gorge, as the slopes in both areas are formed in closely jointed Torlesse greywacke.

The Kaikōura dataset shows that the maximum source area of a single landslide on the coastal Cretaceous greywackes with a slope height of less than 400 m (compared to a maximum slope height of c. 300 m in the Manawatū Gorge) is c. 27,000 m^2. On this basis, the largest landslide likely to occur in the Manawatū Gorge, based on the available data, has a source area covering c. 27,000 m^2.

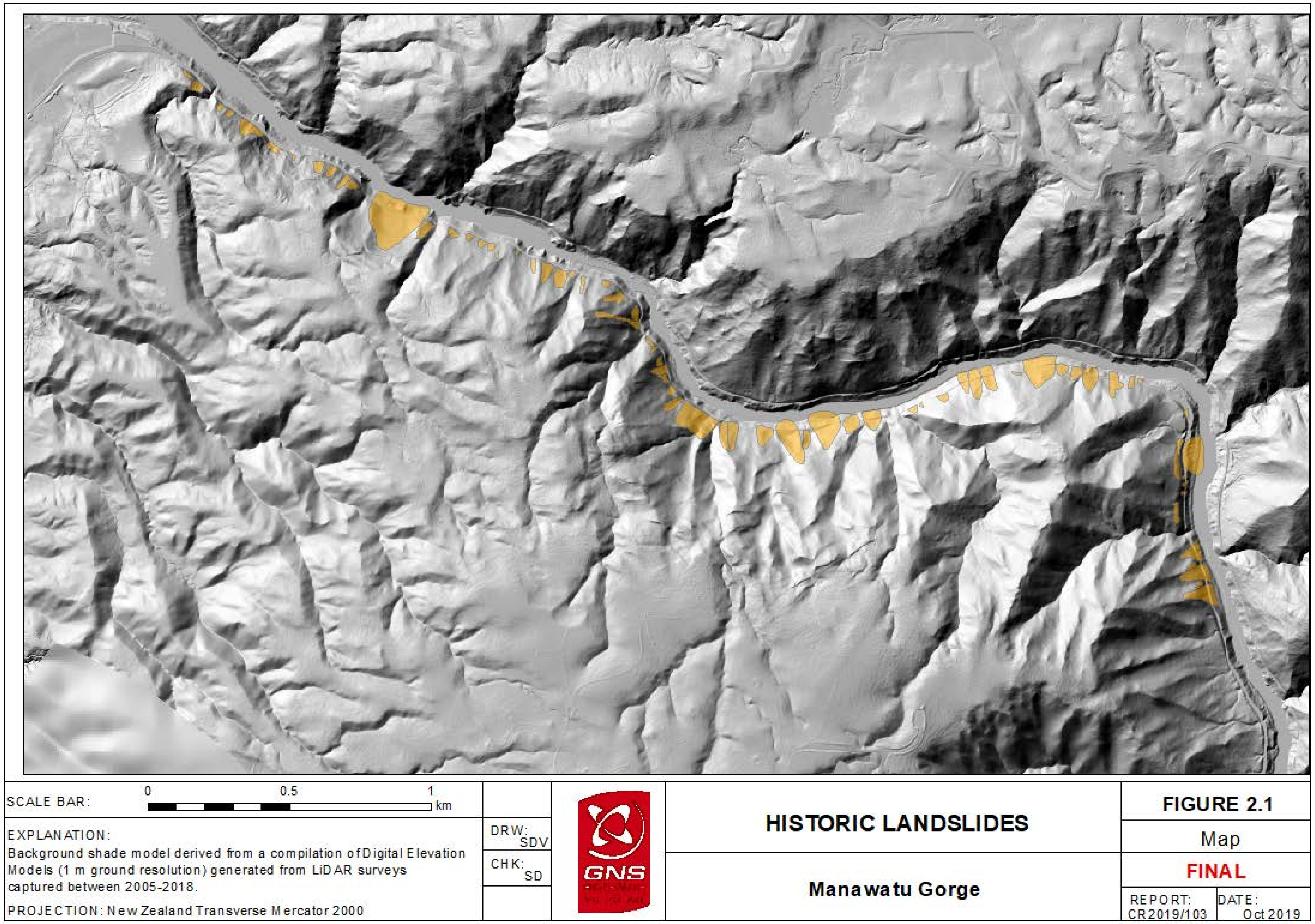

Figure 2.1 Historical mapped landslide inventory for the south side of the Manawatū Gorge (Source: Hancox et al. 2013).

3.0 3D TOPOGRAPHIC STRESS MODELLING

Landslide susceptibility has been inferred from a 3D mechanical model, constructed to estimate slopes where topographic stresses are likely to be greatest. The topographic stress model is 9.3 km x 8.8 km x 1500 m deep and assumes homogeneous Mohr-Coulomb material characteristics (Figure 3.1). The model resolution is a 32 x 32 m grid and the upper surface is displayed as a gridded digital elevation model at that resolution. Because this was an exploratory model, we compiled rock properties from a suite of laboratory experiments conducted on similar materials from the Wellington region (Brideau and Massey 2019). The rock properties used are density = 2560 kg/m^3, bulk modulus = 1.5×10^{10} Pa, shear modulus = 5×10^9 Pa, friction angle = 40°, cohesion = 5×10^5 Pa and tension = 2×10^5 Pa. While this exploratory model provides a useful estimation of the spatial distribution in stress throughout the gorge, more accurate quantification of stress states would require rock properties specific to the Manawatū Gorge. Revising the rock properties would modify the absolute stress values in the model, but the spatial pattern of topographic stresses, as illustrated in Figure 3.1, would remain similar.

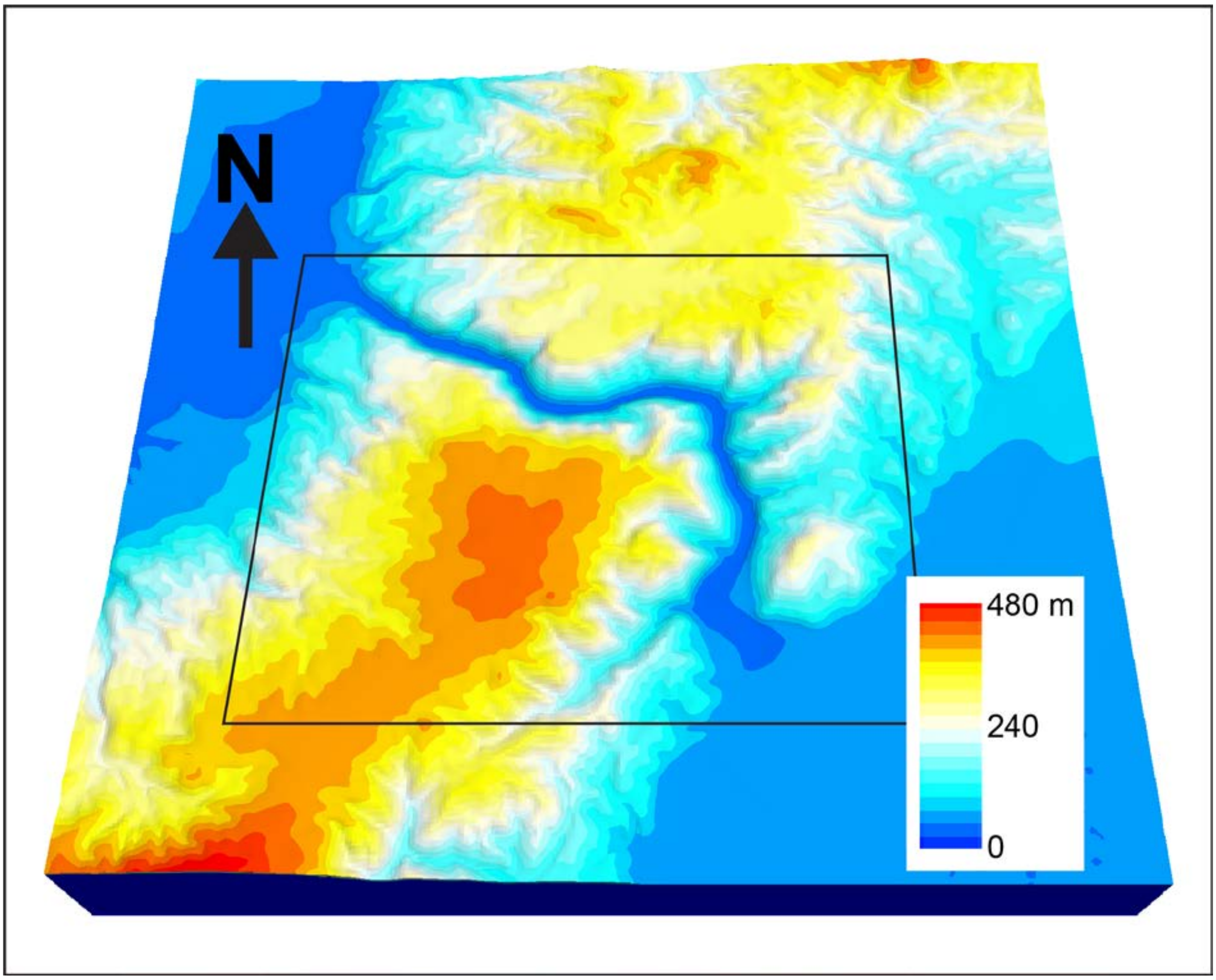

Figure 3.1 Model geometry. 9.3 x 8.8 km at 32 x 32 m grid resolution. Coloured contours are elevation, dark blue = sea level, red = 480 m, interval = 24 m. Box outlines extent shown in Figure 3.2. See text for details of material properties and boundary conditions.

The model is run to equilibrium with the base and sides fixed to determine the stress state within the region, due to the topography and relief (Upton and Sutherland 2014). Shear stresses arise from topographic loading and due to the presence of slopes. The maximum shear stress for each grid cell at the ground surface of the model is shown in Figure 3.2a. The regions of lowest shear stress are on the plains at either end of the gorge and along the low relief at the top of the range either side of the gorge. Shear stresses are greatest where slopes are steep; here, gravity is acting at an angle to the ground surface, which generates a shear stress. The highest shear stresses calculated are within the gorge, indicated in red in Figure 3.2a. As well as the slope steepness, the 3D shape of the topography contributes to the shear stress, which reveals concentrations of shear stress that may not be revealed in 2D cross-sections.

Increasing the shear stress brings the rock closer to failure. In this model, it is the topographic stresses that are moving the rock toward failure. How close a region is to surface failure can be calculated by the stress-strength ratio for each grid cell in the model. Figure 3.2b shows the strength-stress ratio for the Manawatū Gorge. Regions in blue are furthest from failure, dark orange regions are deemed closer to failure. Regions actively undergoing shear failure would show up as red. This combination of model geometry and material properties does not produce regions which are likely to fail under the static topographic load. Sites close to failure (i.e. dark orange) are likely to be the most prone to failure if they experience a stress perturbation, such as an earthquake, or increase in pore pressure due to a heavy rainfall event.

The sites of maximum shear stress in Figure 3.2a (red, orange and yellow), and where the slope stresses are close to the strength in Figure 3.2b (dark orange and orange) on the south side of the Manawatū Gorge, show some correspondence with the historical landslide record shown in Figure 2.1.

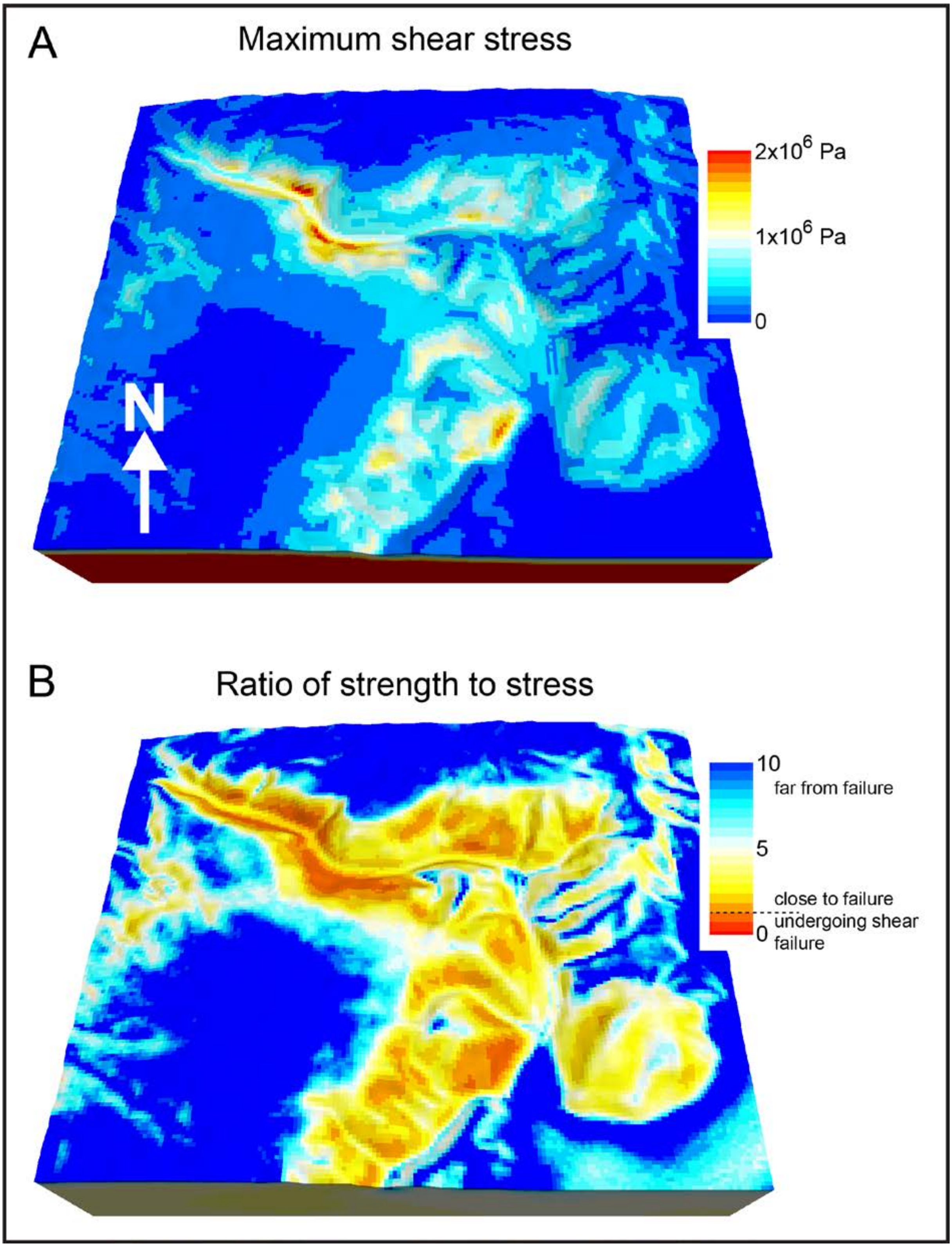

Figure 3.2 Zoom into region shown by box in Figure 3.1. A: Value of maximum shear stress at the surface, in Pascals, through the gorge. Shear stresses are highest at the base of the gorge, where the slopes above are steepest. B: The ratio of strength to stress at the surface of the model. Regions in blue are furthest from failure. Regions in dark orange are closest to failure.

4.0 LANDSLIDE MODELLING

4.1 Cross-Section Development

Previous landslide susceptibility studies in greywacke slopes of the Wellington region indicate that slope angle provides a simple but reliable means of assessing potential landslide susceptibility (Grant-Taylor 1964; Brabhaharan et al. 1994; Hancox et al. 2005; Hancox et al. 2015). As such, slope angle was used to determine which slopes within the Manawatū Gorge were more susceptible to landsliding. The LiDAR-derived Digital Elevation Model (DEM) was used to generate 38 cross-sections equally spaced at intervals of 200 m along the Manawatū Gorge (Figure 4.1). The mean slope angle was calculated from the toe of the slope to the top of the slope (as defined by the break in slope) along the 38 individual cross-sections (Appendix 1). Figure 4.2 displays the slope angles and slope heights in the Manawatū Gorge together with the greywacke slopes in Wellington. The dashed line in Figure 4.2 indicates the maximum slope angles identified for different slope heights, and it is assumed that slopes close to this boundary are therefore the most susceptible to failure. As such, the 10 slopes most susceptible to failure were selected for further landslide failure modelling.

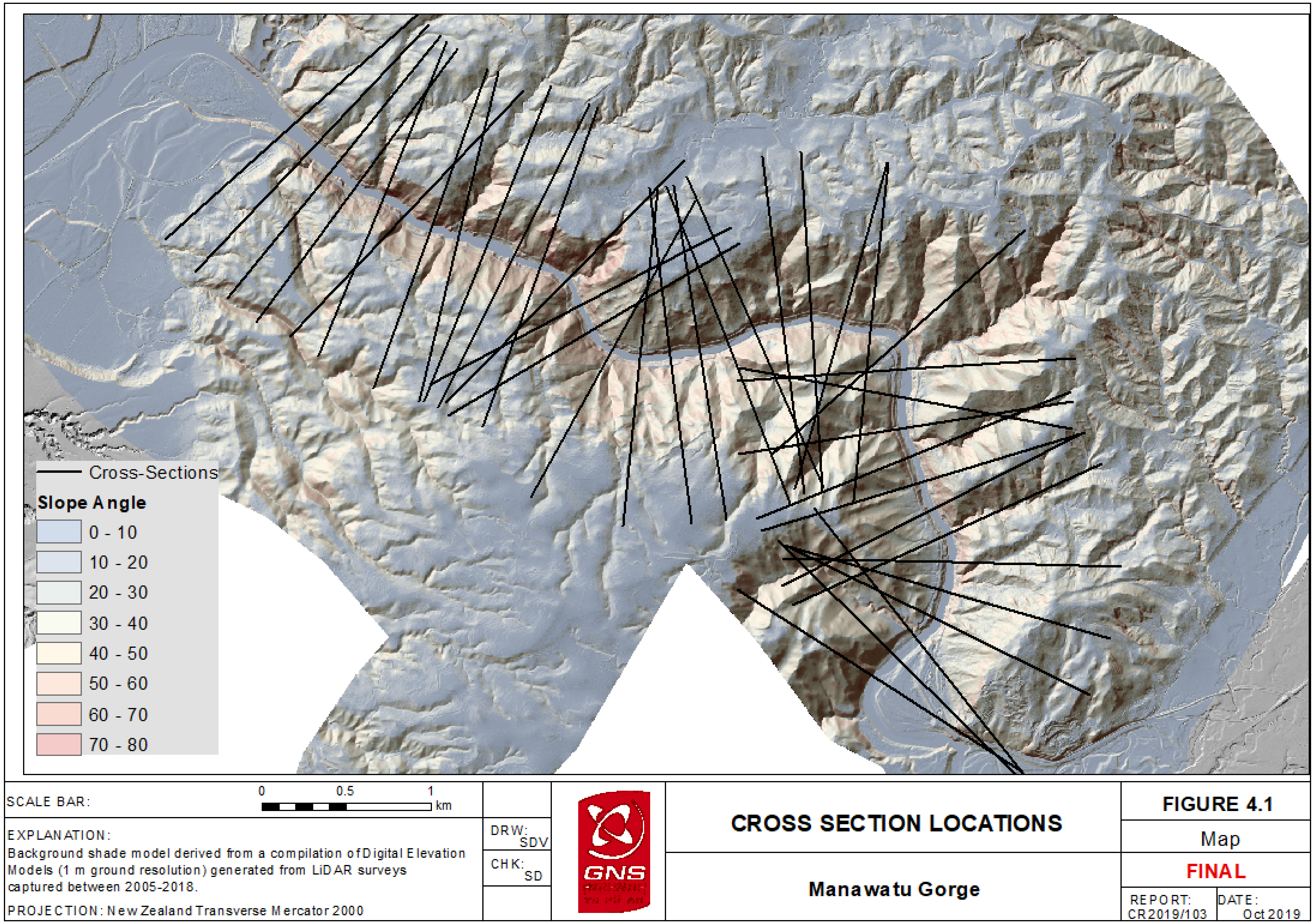

Figure 4.1 Location of 38 cross-sections, equally spaced at 200 m, along the length of the Manawatū Gorge.

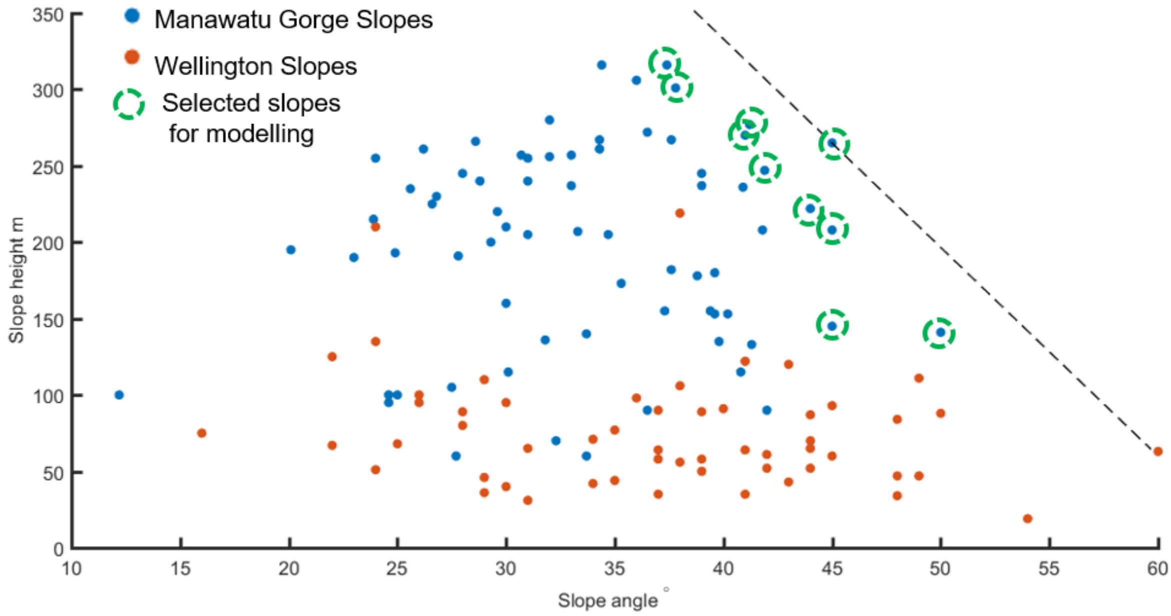

Figure 4.2 Slope angle versus slope height for the 38 different cross-sections in the Manawatū Gorge and data from Wellington greywacke slopes (Hancox et al. 2015). The dashed line represents the upper boundary of slope angles observed in greywacke for both regions. The 10 slopes most susceptible to failure (green dashed circles) were selected for further landslide modelling.

4.2 Landslide Size

As the maximum recorded landslide from both historic Manawatū Gorge records and the greywacke slopes in Kaikōura is 27,000 m^2, the selected modelled landslide size was rounded up to 30,000 m^2 and the geometry was maintained to be a similar shape to historic landslides (Figure 2.1). The 3D topographic stress modelling described in Section 3 of the report was used to help determine the locations of the 10 selected sites for modelling potential landslides in the gorge as displayed in Figure 4.3. Landslide volume estimates generally rely on scaling relationships between landslide volume (V) and landslide area (A), whereby:

$$Landslide\ Volume\ (V) = a.A^{y} \quad \text{Equation 4.1}$$

In this report, the volume area scaling relationship established from Larsen et al. (2010) for New Zealand bedrock was used to calculate the volume from a landslide with an area of 27,000 m^2. This calculation gave a volume of 118,000 m^3.

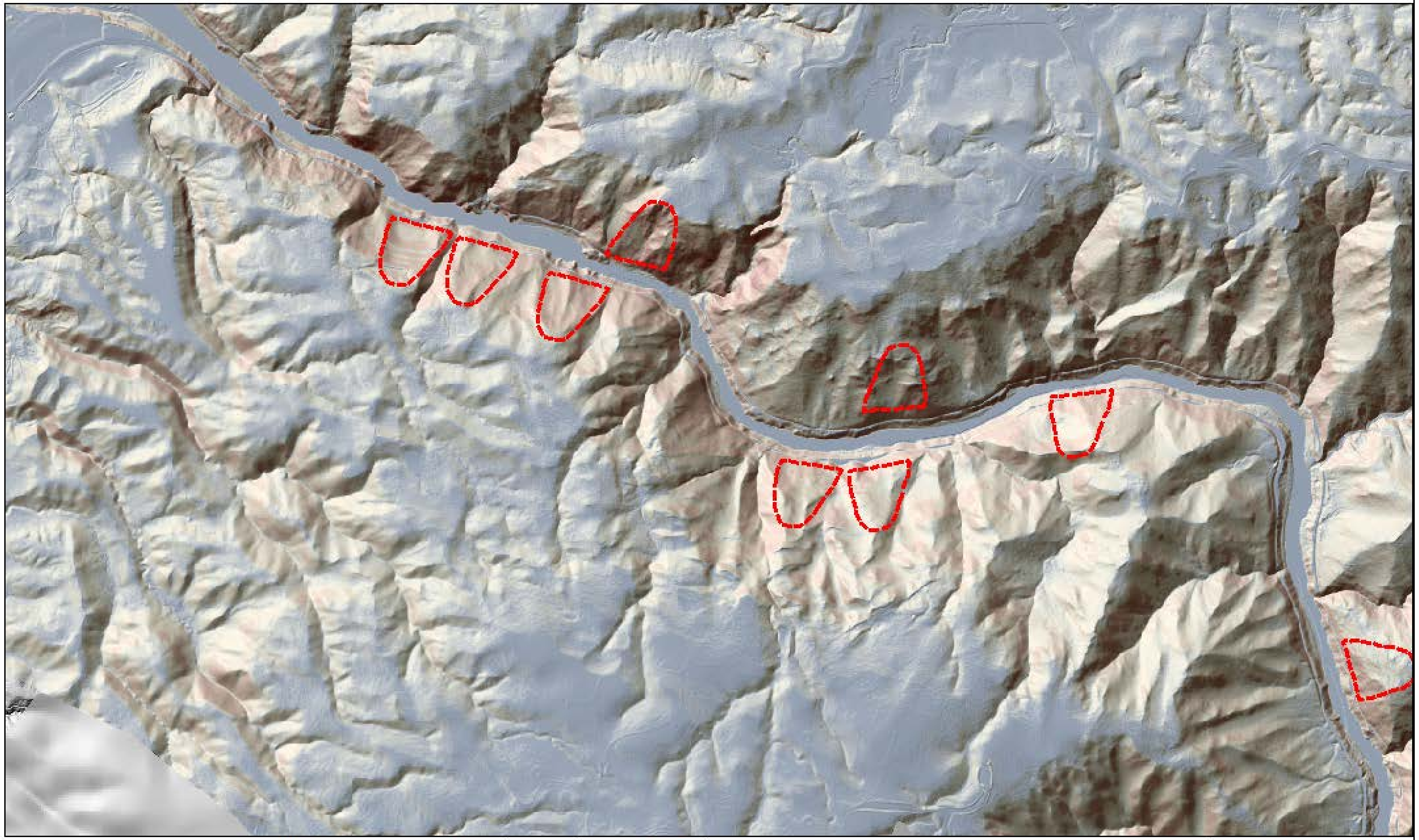

SCALE BAR: 0 0.5 1 km			SOURCE AREAS OF MODELLED LANDSLIDES	FIGURE 4.3
EXPLANATION: Background shade model derived from a compilation of Digital Elevation Models (1 m ground resolution) generated from LiDAR surveys captured between 2005-2018.	DRW: SDV	GNS		Map
	CHK: SD		Manawatu Gorge	FINAL
PROJECTION: New Zealand Transverse Mercator 2000				REPORT: CR2019/103 DATE: Oct 2019

Figure 4.3 Location of the 10 potential landslides along the Manawatū Gorge modelled in this study.

4.2.1 Landslide Runout Modelling

The potential for landslide runout extent, deposit depth and formation of a landslide dam was assessed numerically using the RAMMS software (RAMMS 2011). The software uses slope geometry to evaluate the likely debris runout, area affected, volume, velocity and the maximum and final height of debris in a given location at any moment during the runout. While entrainment of material may occur as the debris moves downslope, this was not included in the simulations conducted for this study.

The physical RAMMS Debris Flow model uses the Voellmy rheology representation of failed landslide material. This model divides the frictional resistance into two parts:

1. a dry-Coulomb type friction (coefficient *μ or Mu*) that scales with the normal stress, and
2. a velocity-squared drag or viscous-turbulent friction (coefficient *xi*) that scale with landslide volume.

It is not possible to physically derive these parameters from testing, but they can be calibrated from the back analysis of well-documented case studies. For this assessment, the RAMMS model parameters were calculated from the back-analysis of 67 debris avalanches (ranging in volume from 300 m^3 to 100 Mm^3) published in the literature, including several debris avalanches that occurred on the range front in the Southern Alps. These are the Maruia (McSaveney et al. 2014), Round Top (large) and Round Top (small) (Wright 1998) debris avalanches.

The modelled parameters *mu* (*μ*) and *xi* used for landslide forecasting were derived by fitting a power law to the data (Figure 4.4). The values used for forecasting the runout of debris avalanches and flows of a given source volume are listed in Table 4.1. The results from the back-analysis show that the RAMMS model parameters are sensitive to the initial volume of the landside, where the *Mu* and *xi* parameters decrease with increasing source volume, which relates to a decrease in the 'viscosity' of the flowing mass.

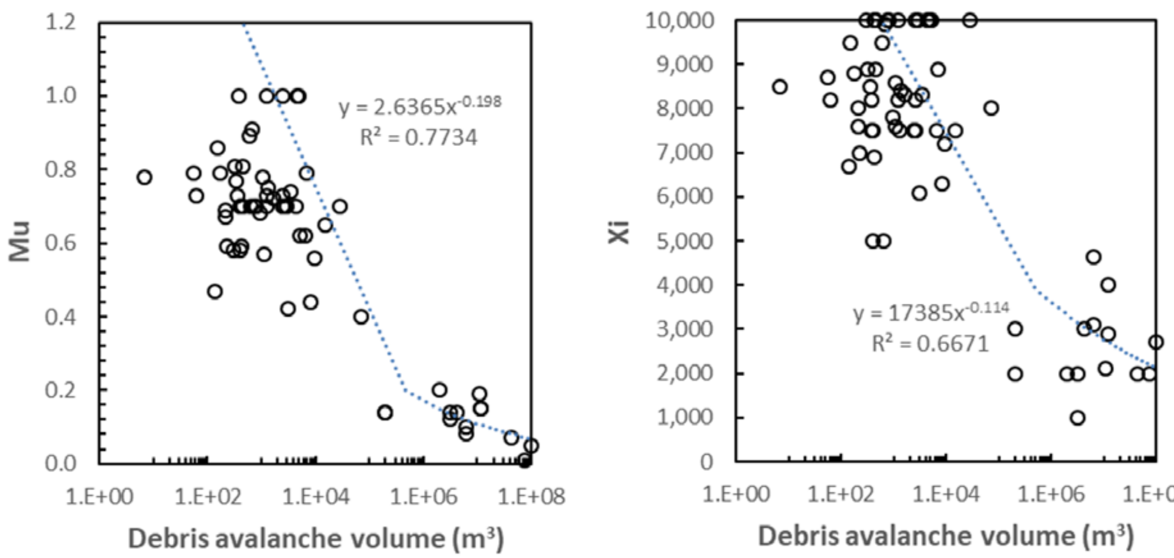

Figure 4.4 Debris flow: the range of parameters used to back-analyse the runout of debris flows published in the literature (n = 67), using the RAMMS software.

Table 4.1 RAMMS model parameters used for forecasting debris avalanche runout.

Representative Landslide Volume (m^3)	Debris Avalanche Forecast Parameters	
	Mu (μ)	***Xi***
10,000	0.4	10,000
50,000	0.3	50,000
100,000	0.3	100,000
120,000	0.3	120,000

Cross-sections through each simulated landslide deposit for each of the 10 selected slopes are provided in Appendix 2. The minimum height of the deposit in the valley was manually calculated from these cross-sections. This height (the minimum breach height) was used as the height of the modelled landslide dams. From analysis of the landslide cross-sections (Appendix 2) the minimum breach height was close to, but did not exceed, 10 m for all cross-sections. A 10 m minimum breach height was therefore used in our landslide dam breach modelling.

4.2.1.1 Sensitivity Analysis

Sensitivity analysis was undertaken on the RAMMS parameters as the modelling was unable to recreate the landslide deposit morphology previously observed in the Manawatū Gorge. Recent failures in the Manawatū Gorge have a cone-like deposit shape (Figure 4.5), while the cross-sections from the RAMMS model simulations (Appendix 2) flowed across the valley and produced a thicker deposit on the opposite slope.

To assess whether the field observations of landslide deposit shape could be replicated, the RAMMS parameters were adjusted. These adjusted parameters are outlined in Table 4.2 and the cross-sections of the various resulting deposits for one selected landslide source (Mid Gorge 1 – Appendix 2) are displayed in Figure 4.6. In several of the models, the friction parameters of the valley floor were adjusted to reflect the presence of 'softer' ground (i.e. alluvial and colluvial river material), which may have the potential to absorb energy and therefore change the runout extent and shape. Additionally, the momentum energy cut-off was adjusted. This represents the stopping criteria, as determined from classical mechanics where momentum is the product of the mass and velocity of an object.

While these adjustments to the RAMMS parameters changed the cross-sectional shape of the landslide deposit, they did not ultimately result in a large difference in minimum deposit height (or dam breach height) in the valley floor. However, it is worth noting that further numerical analysis, along with better replication of observed landslide deposits in the valley, will decrease the uncertainty associated with this minimum dam breach height.

Figure 4.5 A landslide failure during 2011 in the Manawatū Gorge, displaying a cone-like deposit shape (Source: GT Hancox).

Table 4.2 Adjusted RAMMS parameters used for forecasting debris avalanche runout to produce a cone-like geometry.

Model Simulations	**Debris Avalanche Forecast Parameters**		**Friction Parameters of Valley Floor**		**Momentum Energy Cut-Off (%)**
	Mu (μ)	***Xi***	***Mu (μ)***	***Xi***	
16	0.3	4,600	0.1	16	0.3
16a	0.3	4,600	NA	16a	0.3
16b	0.3	4,600	0.1	16b	0.3
16c	0.3	4,600	NA	16c	0.3
16d	0.3	4,600	0.1	16d	0.3
16e	0.3	5,400	NA	16e	0.3

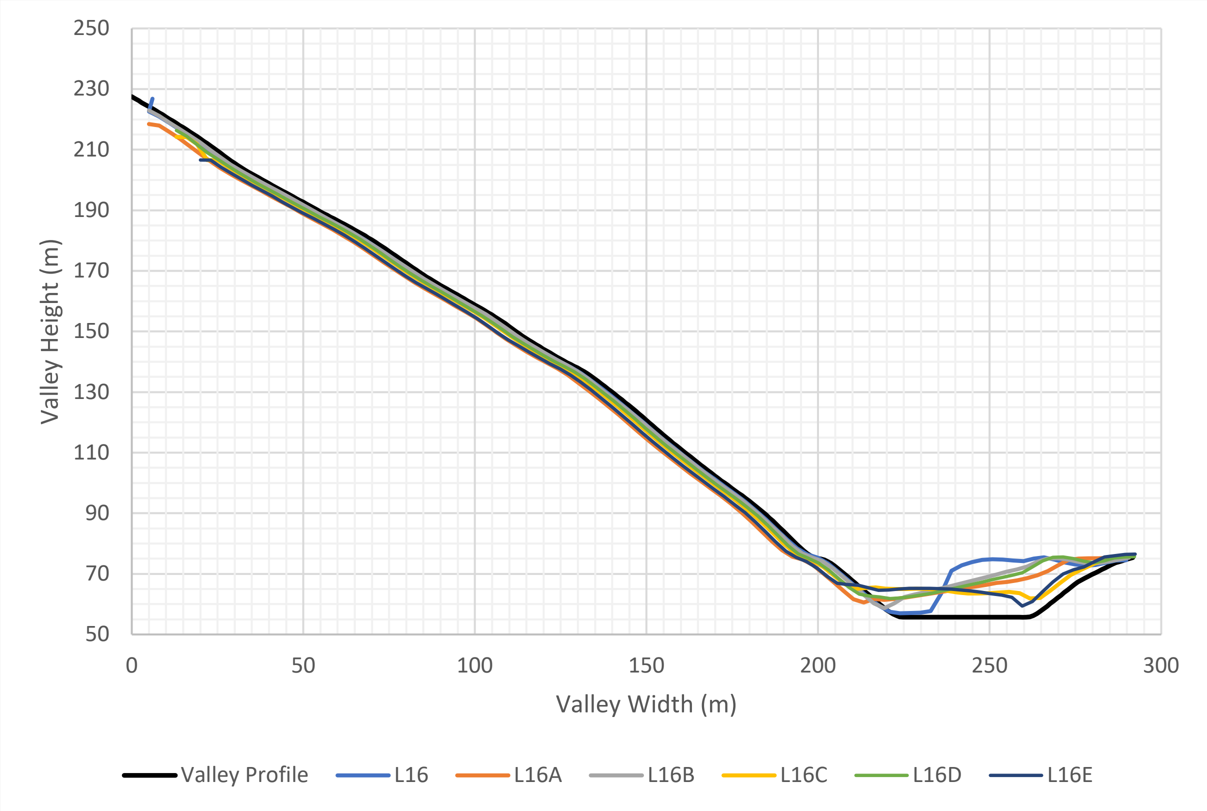

Figure 4.6 Landslide deposit cross-sections for different model simulations of the same potential landslide location.

5.0 LANDSLIDE DAM MODELLING

5.1 Landslide Dam Heights

From analysis of the landslide cross-sections (Appendix 2) and the sensitivity analysis, the minimum breach height was approximately 10 m for all cross-sections. This 10 m breach height was therefore used in our landslide dam breach modelling. To evaluate the potential impact of a much larger landslide dam, a dam height of 20 m was also calculated. The results from modelling a 20 m dam height are not included in this report, as they are considered unrealistic scenarios based on empirical data from historical landslide sizes in similar greywacke terrain. As the modelled landslides clustered in three areas within the gorge (Figure 4.3), landslide dam breach simulations were undertaken for the lower section, middle section and upper section of the gorge separately using dam heights of 10 m and 20 m, respectively.

5.2 Dam Longevity

The probability of failure of a landslide dam was assessed using the Dimensionless Breach Index (DBI) as described in Ermini and Casagli (2003). Using this method, the probability of dam failure is calculated using the dam volume and dam height and the upstream catchment area (Figure 5.1). A dam height of 10 m was calculated from RAMMS modelling and a dam volume 120,000 m^3 was determined from the landslide area scaling relationship analysis. The catchment area of the Manawatū River, upstream of the Manawatū Gorge, was measured at 3200 km^2 using shapefiles from the Ministry for the Environment's river environment classification tool found here: https://data.mfe.govt.nz/layer/51845-river-environment-classification-new-zealand-2010/history/ (accessed 10th June 2019).

The DBI for a landslide dam in the Manawatū Gorge indicates a 90% probability of failure (Figure 5.1). Similar landslide dams formed in greywacke terrain after the 2016 Kaikōura Earthquake are also plotted for comparison. The only landslide dam with an upstream catchment area similar in size to the catchment area occurred on the Clarence River. This dam failed 16 hours after the Kaikōura Earthquake and infers that a landslide dam in the Manawatū Gorge should be similarly short-lived.

5.3 Upstream Flooding Extent

The upstream lake extent of landslide dams at three locations along the gorge has been modelled using the compiled LiDAR data (Figures Figure 5.2 to Figure 5.4). Models of flooding behind a 10 m high dam located in the lower, middle and upper sections of the gorge indicates that the lakes would mainly be confined to either existing or previous channels.

From the RAMMS modelled deposit heights, the lowest point where a dam could be over-topped was taken as the dam height. The volume of the lake was calculated as the maximum lake volume which could form upstream. This was calculated by projecting a horizontal plane upstream which was set at the elevation of the lowest point on the dam crest. The edges of the simulated lake were then defined as the point where the projected plane intersects the DEM. The lake volumes were calculated by differencing the simulated lake from the DEM. The potential energy of the stored water was then a function of dam height, lake volume, gravity and the density of water.

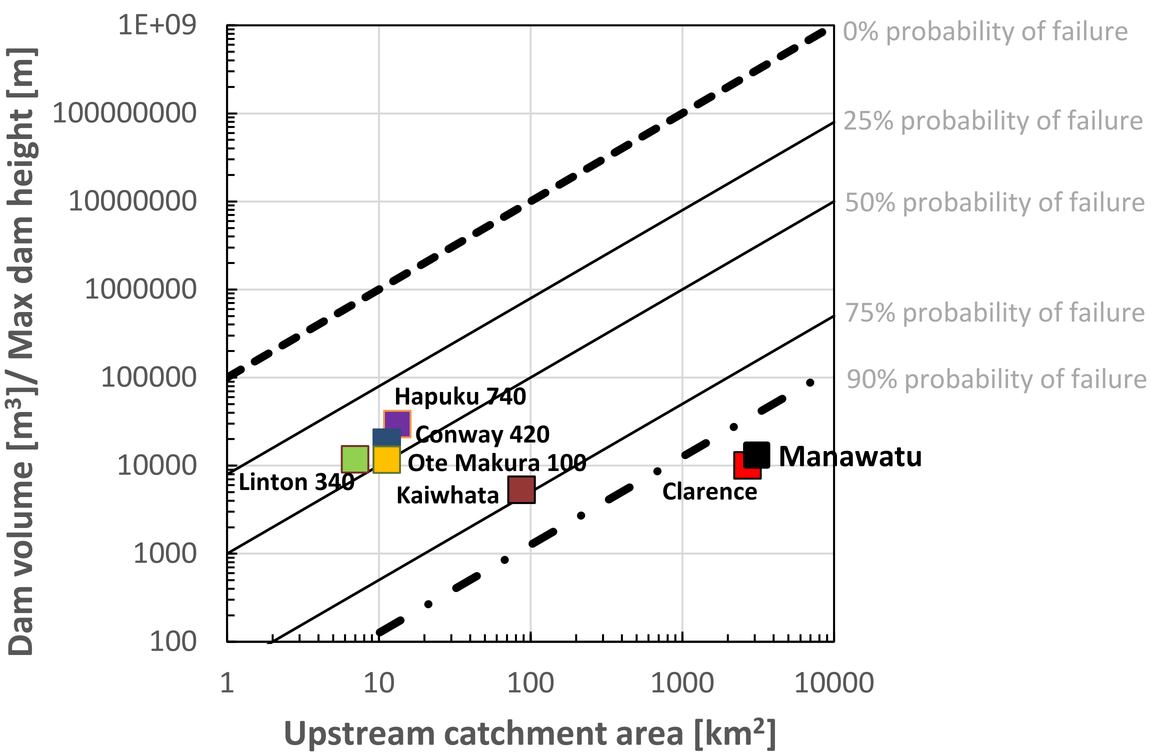

Figure 5.1 Dimensionless Breach Index (Ermini and Casagli 2003) showing New Zealand greywacke landslide dam examples from the 2016 Kaikōura Earthquake and a modelled Manawatū Gorge landslide dam. The 2019 Kaiwhata dam near the Wairarapa coast on the territorial boundary between Masterton and Carterton Districts is included because it is a recent event and the consequences of rapid failure were accurately forecast (conservatively) by the techniques used in this study.

Table 5.1 Summary of the input parameters required to run the RAMMS simulations.

Location	Dam Height (m)	Cross-Sectional Dam Area (m²)	Volume of Dam (m³)	Volume of Water (Mm³)	Total Volume (Mm³)	Calculated Velocity of Water Outflow (m/s)	Empirical Qmax – Discharge (m³/s)
Lower Gorge	10	300	150,000	2.0	2.2	2.4	700
Lower Gorge	20	1300	650,000	167.0	167.7	4.5	5,900
Mid Gorge	10	375	206,250	2.9	3.1	2.2	800
Mid Gorge	20	1500	825,000	163.0	163.9	3.9	5,800
Upper Gorge	10	300	165,500	3.9	18.3	3.1	900
Upper Gorge	20	750	412,500	38.4	38.8	4.1	3100

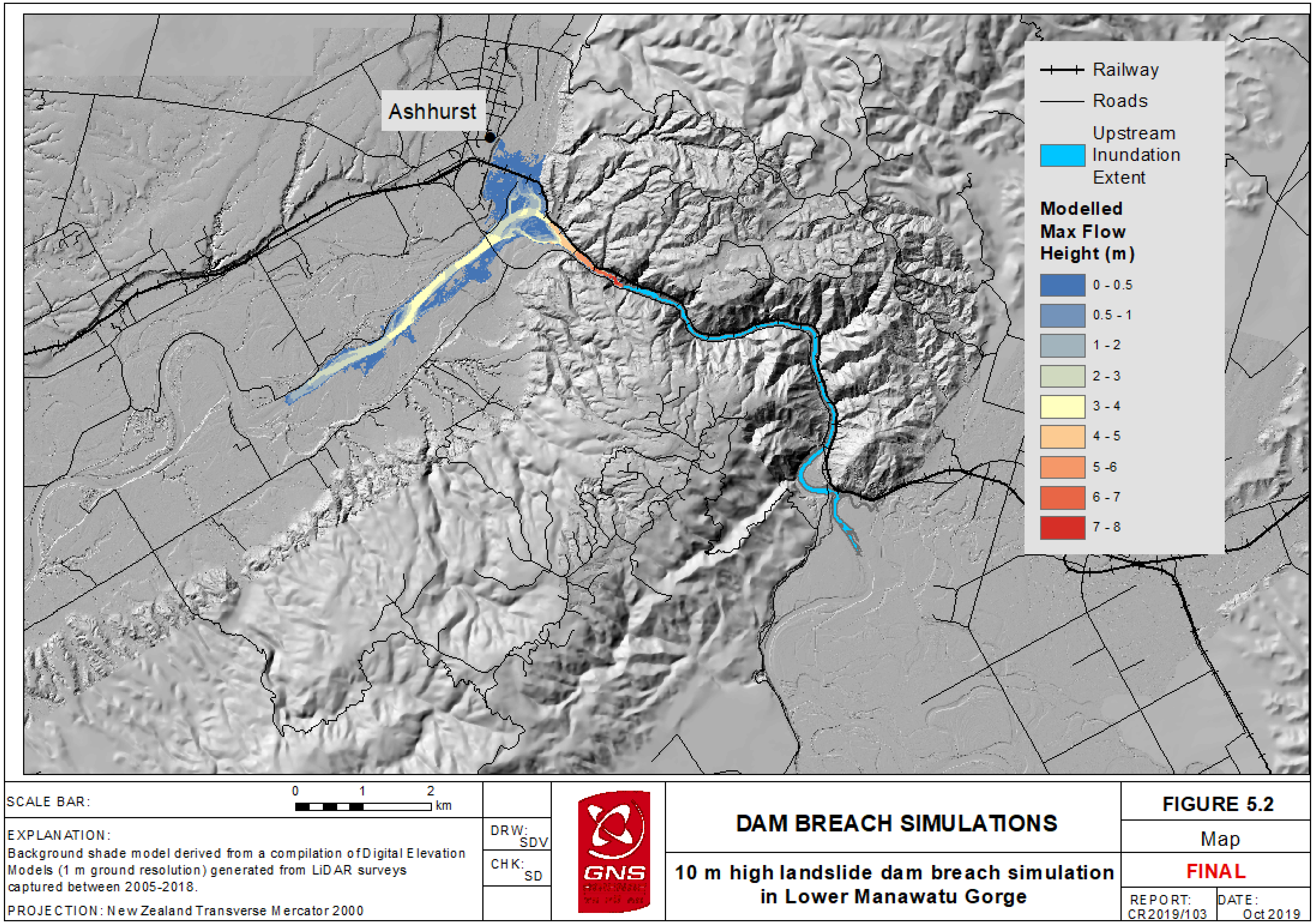

Figure 5.2 Modelled upstream inundation and downstream flooding of a 10 m high dam located in the lower Manawatū Gorge.

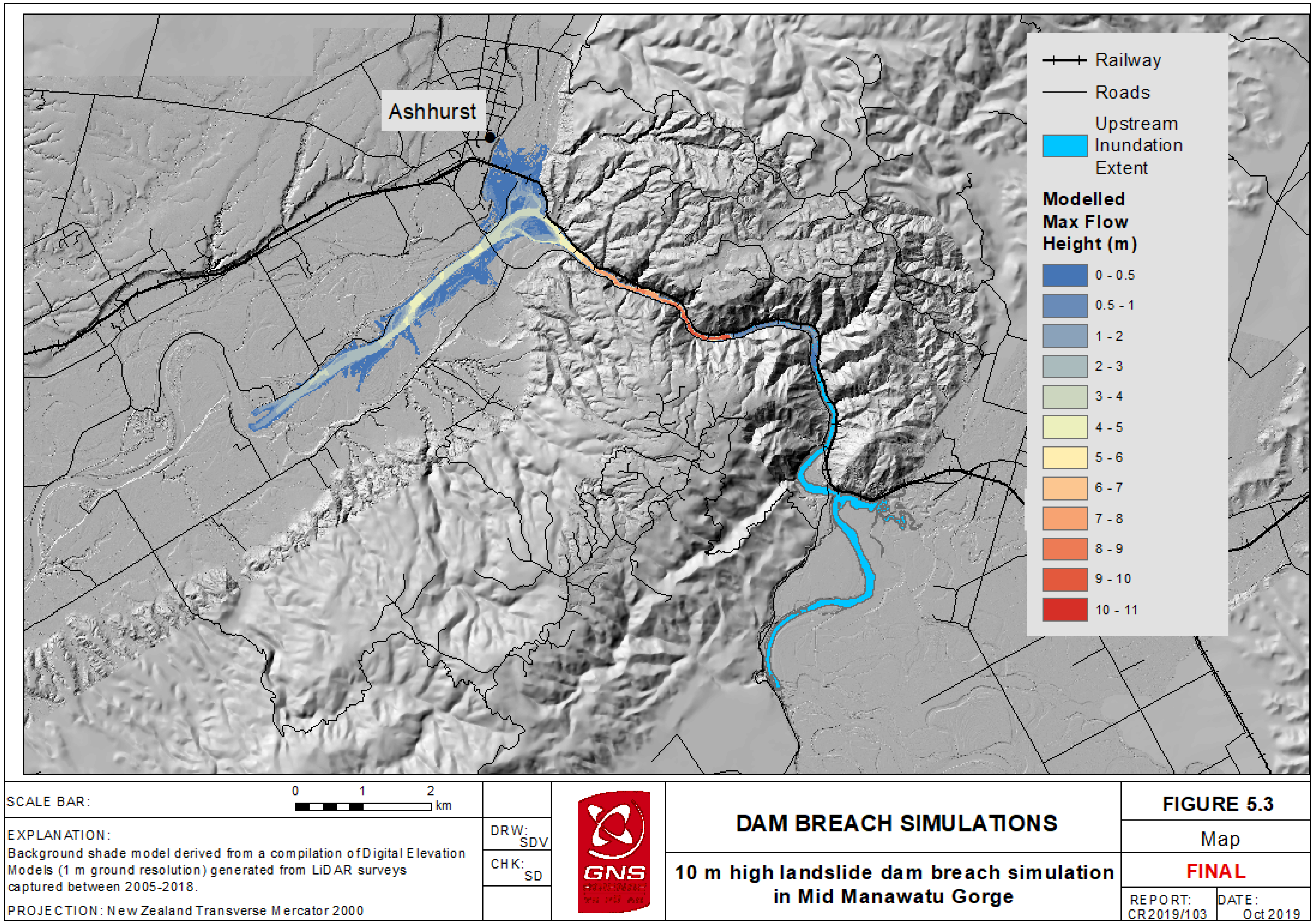

Figure 5.3 Modelled upstream inundation and downstream flooding of a 10 m high dam located in the middle Manawatū Gorge.

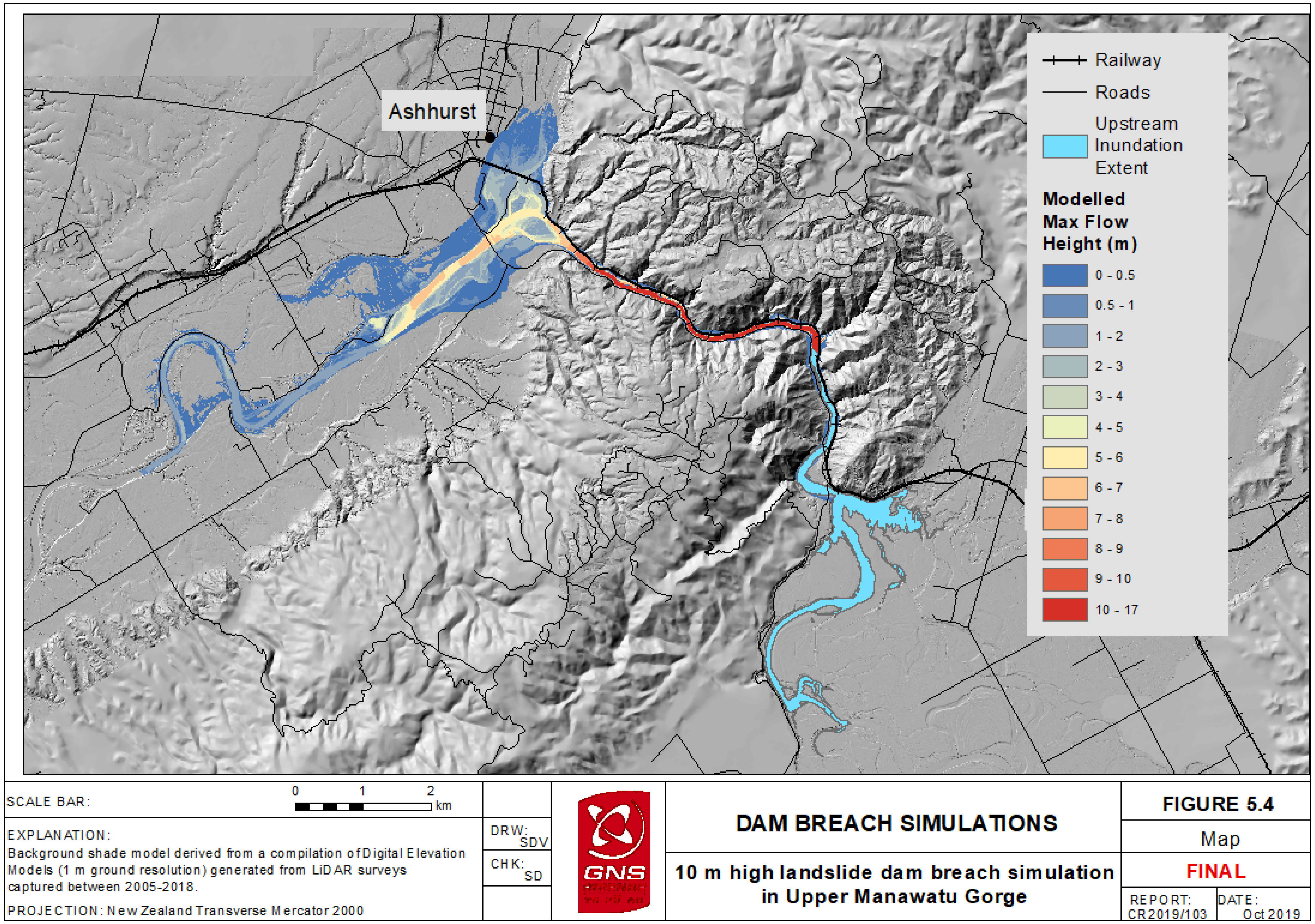

Figure 5.4 Modelled upstream inundation and downstream flooding of a 10 m high dam located in the upper Manawatū Gorge.

5.4 Numerical Analysis

Landslide dam breaches were simulated using the RAMMS debris flow software. Within the software, the water outflow from a dam breach event is modelled using a basic three-point hydrograph. In this hydrograph, the maximum discharge occurs at time (t) 1, immediately after the breach occurs, and then decreases through time until zero discharge is achieved at t2 (Figure 5.5). The hydrograph requires input of the discharge rate, velocity of water and time taken for the lake to drain. Frictional input parameters are required, and these are set to represent the frictional properties of water. As such, *mu* is set to 0.01, and *xi* is set to 100 m/s^2.

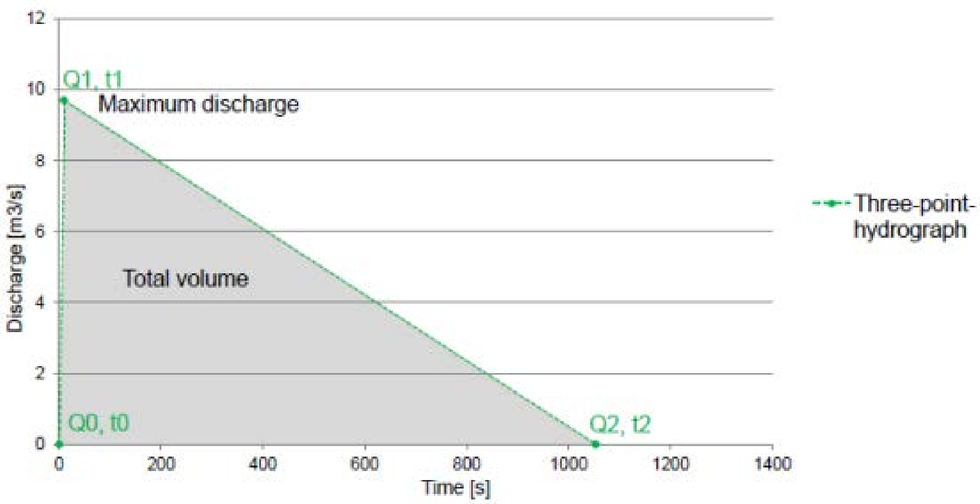

Figure 5.5 Conceptual three-point hydrograph model (RAMMS 2011). Discharge rate = Q; time = t.

The potential maximum discharge rate (Qmax) was estimated from literature regression equations. These regression equations (Costa and Schuster 1988; Costa 1985; Walder and O'Connor 1997) use either the dam height and volume of the impounded lake (reservoir) or the potential energy of stored water to calculate the estimated discharge rate. The average estimated rate determined from these seven equations was used as the discharge rate in the models (Table 5.2).

Table 5.2 Regression relationships to calculate maximum discharge rate (Qmax) for landslide dam breaches from dam height (D), lake volume (V_0) and the potential energy of the stored water (E_p).

Reference	Equation	No. of Data Points	r^2
Costa and Schuster (1988)	$Qmax = 0.0158E_p^{0.41}$	12	0.81
Costa (1985)	$Qmax = 672(V_0/10^6)^{0.56}$	10	0.73
Costa (1985)	$Qmax = 6.3D^{1.59}$	10	0.74
Costa (1985)	$Qmax = 181(DV_o/10^6)^{0.43}$	10	0.76
Walder and O'Connor (1997)	$Qmax = 1.6V_0^{0.46}$	19	0.6
Walder and O'Connor (1997)	$Qmax = 6.7D^{1.73}$	19	0.82
Walder and O'Connor (1997)	$Qmax = 0.99DV_o^{0.40}$	19	0.7

The assumed velocity of the water discharge was calculated as a function of the discharge rate divided by a simplistic triangular cross-sectional area of the dam. This cross-sectional area was calculated from the minimum dam height and the existing topography of the valley (Table 5.2Table 5.2). The estimated time taken for the lake to drain (i.e. between t1 and t2; Figure 5.5) is calculated as a function of both dam and lake area, as well as the discharge rate within the RAMMS software.

5.5 Downstream Outflow Extent

Figures Figure 5.2 to Figure 5.4 display the downstream flooding extent and flow heights of a 10 m high dam located in the lower, middle and upper sections of the gorge, respectively. The 10 m high dam in the upper gorge inundates a larger area than equivalent dams in the lower and middle gorge and, as a result, the lake behind a landslide dam in the upper gorge has a larger lake volume (Table 5.1). This larger lake volume produces a more extensive flood when the dam fails (c.f. Figures Figure 5.2 to Figure 5.4).

6.0 DISCUSSION

The potential impacts of a large landslide damming the Manawatū Gorge have been investigated. Empirical evidence from greywacke slopes in similar terrain indicates that the largest credible landslide likely to form in the Manawatū Gorge has an area of 27,000 m^2 and volume (based on area to volume scaling relationships) of 118,000 m^3. These values are consistent with the largest historical landslide in the gorge. Topographic stress modelling of the Manawatū Gorge indicates that the most susceptible slopes to failure are also in broad agreement with the historical record of landslides, and 10 of these sites were chosen for further analysis.

RAMMS runout modelling at all 10 sites indicates a consistent minimum dam height of 10 m regardless of its location (upper, middle, lower) with the gorge. These landslides have then been used to establish the minimum height of a landslide dam and to determine the maximum extent of upstream flooding and the volume of water available to contribute to a debris flood downstream should the dam fail rapidly.

The location of the dam within the gorge determines the extent of flooding both upstream and downstream. At a dam crest height of 10 m, upstream flooding will not reach Woodville from the most upstream of the 10 modelled dams. Downstream flooding from rapid failure of the modelled dams may reach the low river terrace below Ashhurst. Despite this, the township is unlikely to be affected, as Ashhurst is built on a higher terrace and is protected from flooding in the Pohangina and the Manawatū Rivers. Flooding is unlikely to affect Palmerston North beyond the confines of flood protection adjacent to the Manawatū River.

The longevity of a landslide dam forming in the Manawatū Gorge was assessed using the DBI. This method indicates that a landslide dam forming in the Manawatū Gorge has a 90% chance of failing. Based on the behaviour of a similar landslide dam on the Clarence River, which failed 16 hours after the Kaikōura Earthquake, it is anticipated that a landslide dam in the Manawatū Gorge should be similarly short-lived.

One limitation to the work presented here is that the flood modelling results are relatively coarse, and more detailed flood route modelling by Horizons Regional Council river engineers and hydrologists may refine the extent and routing of downstream flooding.

A second limitation for the work carried out to date is the inability of the landslide modelling software to replicate the expected geometry of typical large landslides in greywacke terrain in the Manawatū Gorge (c.f. Figures Figure 4.5 and Figure 4.6). The 2011 landslide in the Manawatū Gorge (Figure 4.5), which is similar in area and volume to the landslides modelled in this report, did not result in a landslide dam in the gorge. This observation and other elements of conservatism in the methodology (considering only slopes up to 400 m high in the Kaikōura dataset; landslide dam heights of only 10 m during landslide modelling) provide confidence that the results presented in this report are appropriately conservative.

Interferometric Synthetic-Aperture Radar (InSAR) remote sensing acquisitions could help inform the likelihood and constrain the size of a large landslide occurring in the Manawatū Gorge. InSAR acquisition over several years could determine if the slopes of the Manawatū Gorge are moving and, if so, where and at what rate (a minimum of two dates are required for this) and whether the movement rates are accelerating (a minimum of three or more dates required). This would supplement the work carried out in this study and allow the need for future work to be prioritised in different areas of the gorge as appropriate.

7.0 CONCLUSIONS AND RECOMMENDATIONS

7.1 Conclusions

The following conclusions can be made based on the results from this study:

- Empirical evidence shows that the largest landslide (maximum credible event) likely to form in the Manawatū Gorge, based on the historical performance of slopes in the Manawatū Gorge and similar slopes elsewhere (Wellington and Kaikōura), has an area of 27,000 m^3.
- Area-volume scaling relationships provide for a landslide volume of 118,000 m^3 for a maximum landslide area of this size.
- A landslide of this volume could potentially form a dam on the Manawatū River with a minimum crest height of no more than 10 m. However, the typical geometry of a large landslide in the Manawatū Gorge greywacke could not be replicated by the modelling software.
- Upstream flooding will not reach Woodville from the most upstream of the modelled landslide dams.
- Downstream flooding from rapid failure of the modelled dams, with a dam crest height of 10 m, may reach the low river terrace below Ashhurst. But, as Ashhurst is built on a higher terrace and is protected from flooding in the Pohangina and the Manawatū Rivers, the township is unlikely to be affected.
- Flooding is unlikely to affect Palmerston North beyond the confines of flood protection adjacent to the Manawatū River.
- A landslide dam in the Manawatū Gorge has a 90% chance of failing.
- Based on the behaviour of a similar landslide dam on the Clarence River, which failed 16 hours after the Kaikōura Earthquake, there is an expectation that a landslide dam in the Manawatū Gorge would be similarly short-lived.

7.2 Recommendations

The following recommendations for follow-up and future work are made:

- Horizons Regional Council river engineers can use the data supplied with this report to refine the upstream and downstream flooding impacts.
- Repeat remote sensing acquisitions (e.g. InSAR) are used over several years to determine if the slopes of the Manawatū Gorge are moving and, if so, where and at what rate (a minimum of two dates required) and whether the movement rates are accelerating (a minimum of three or more dates required).
- The modelling work is reviewed in 10 years to assess the results of this study using updated tools and data.

8.0 ACKNOWLEDGEMENTS

The authors acknowledge the review contributions of Ramon Strong (Horizons Regional Council), Marc-André Brideau and Jon Carey (GNS). Horizons Regional Council is thanked for the supply of both Horizons Regional Council and NZTA LiDAR data for the Manawatū Gorge.

9.0 REFERENCES

Brabhaharan P, Hancox GT, Dellow GD, Perrin ND. 1994. Earthquake induced slope failure hazard study, Wellington Region. Wellington (NZ): Wellington Regional Council. 6 vol.

Brideau M-A, Massey CI. Forthcoming 2019. SLIDE (Wellington): Review of geomechanical data for greywacke in the Wellington Region. Lower Hutt (NZ): GNS Science. (GNS Science report; 2019/39).

Costa JE. 1985. Floods from dam failures. Denver (CO). U.S. Geological Survey. 54 p. Open-File Report 85-560.

Costa JE, Schuster RL. 1988. The formation and failure of natural dams. *GSA Bulletin.* 100(7):1054–1068. doi:10.1130/0016-7606(1988)100<1054:TFAFON>2.3.CO;2.

Ermini L, Casagli N. 2003. Prediction of the behaviour of landslide dams using a geomorphological dimensionless index. *Earth Surface Processes and Landforms.* 28(1):31–47. doi:10.1002/esp.424.

Grant-Taylor TL. 1964. Stable angles in Wellington greywacke. *New Zealand Engineering.* 19(4):129–130.

Hancox GT, Dellow GD, Perrin ND, McSaveney MJ. 2005. Western Corridor transportation study: review of geological hazards affecting the proposed Coastal Highway upgrade and Transmission Gully motorway route. Lower Hutt (NZ): Institute of Geological & Nuclear Sciences Limited. 62 p. Client Report 2005/161. Prepared for Porirua City Council.

Hancox GT, McSaveney MJ, Davies TR, Hodgson K. 1999. Mt Adams rock avalanche of 6 October 1999 and the subsequent formation and breaching of a large landslide dam in Poerua River, Westland, New Zealand. Lower Hutt (NZ): Institute of Geological & Nuclear Sciences. 22 p. (Institute of Geological & Nuclear Sciences science report; 99/19).

Hancox GT, Perrin ND, Lukovic B, Massey CI. 2015. Quantifying the seismic response of slopes in Christchurch and Wellington: Wellington slope types and characterisation. Lower Hutt (NZ): GNS Science. 106 p. (GNS Science report; 2013/58).

Hancox GT, Robson CD, Lukovic B. 2013. Engineering geological assessment of the risk and potential magnitude of future landslides that might close SH3 within the Manawatu Gorge. Lower Hutt (NZ): GNS Science. 77 p. Consultancy Report 2012/254. Prepared for New Zealand Transport Agency (NZTA).

Larsen IJ, Montgomery DR, Korup O. 2010. Landslide erosion controlled by hillslope material. *Nature Geoscience.* 3:247–251.

Massey CI, Townsend DB, Rathje E, Allstadt KE, Lukovic B, Kaneko Y, Bradley B, Wartman J, Jibson RW, Petley DM, et al. 2018. Landslides triggered by the 14 November 2016 Mw 7.8 Kaikoura earthquake, New Zealand. *Bulletin of the Seismological Society of America*. 108(3B):1630–1648. doi:10.1785/0120170305.

McSaveney MJ, Cox SC, Hancox GT. 2014. Seeking a credible cause of the recent increase in rock-avalanche frequency in New Zealand's Southern Alps [abstract]. In: *AGU Fall Meeting*; 2014 Dec 15–19; San Francisco, CA. Washington (DC): American Geophysical Union. Abstract NH41A-3775.

RAMMS. 2011. RAMMS - rapid mass movements simulation, A numerical model for debris flows in research and practice, User Manual v1.7.0, Debris Flow. November 2017 update. Davis Dorf (CH): WSL Institute for Snow and Avalanche Research SLF. 1–116.

Upton P, Sutherland R. 2014. High permeability and low temperature correlates with proximity to brittle failure within mountains at an active tectonic boundary, Manapouri tunnel, Fiordland, New Zealand. *Earth and Planetary Science Letters.* 389:176–187. doi:10.1016/j.epsl.2013.12.032.

Walder JS, O'Connor JE. 1997. Methods for predicting peak discharge of floods caused by failure of natural and constructed earthen dams. *Water Resources Research.* 33(10):2337–2348. doi:10.1029/97WR01616.

Wright CA. 1998. The AD 930 long-runout Round Top debris avalanche, Westland, New Zealand. *New Zealand Journal of Geology and Geophysics.* 41(4):493–497. doi:10.1080/00288306.1998.9514826.

APPENDICES

This page left intentionally blank.

APPENDIX 1 INDIVIDUAL CROSS SECTIONS

Section locations shown on Figure 4.1. Numbered from downstream (LT1) to upstream (LT39).

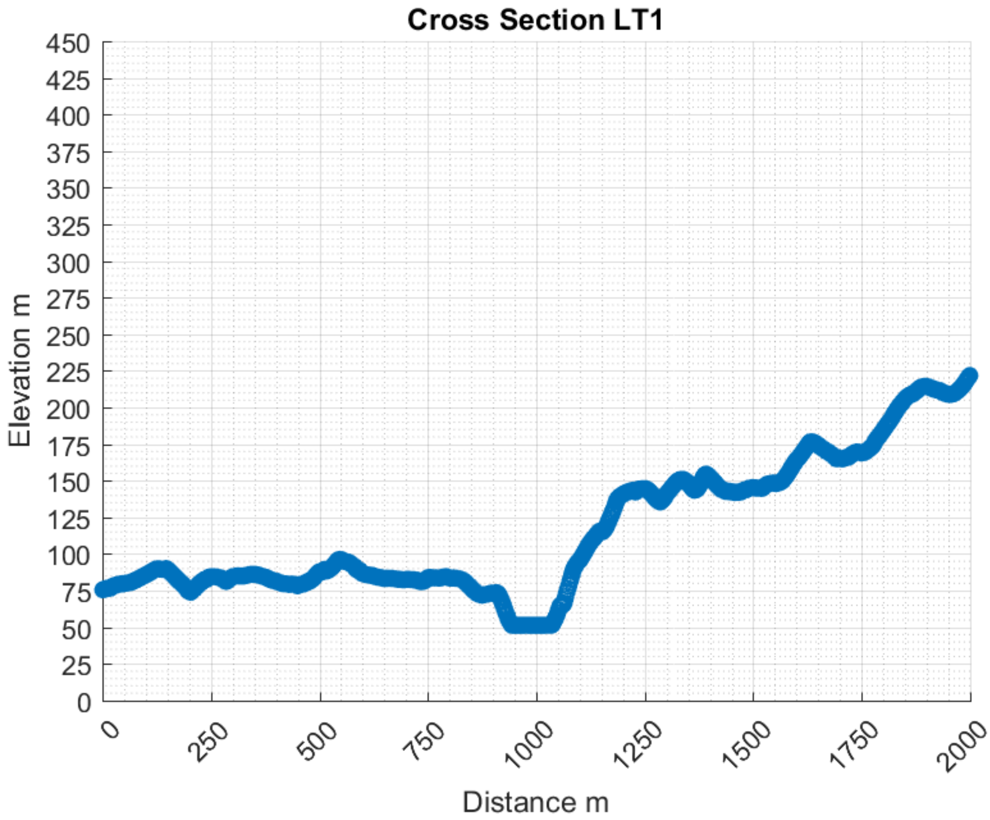

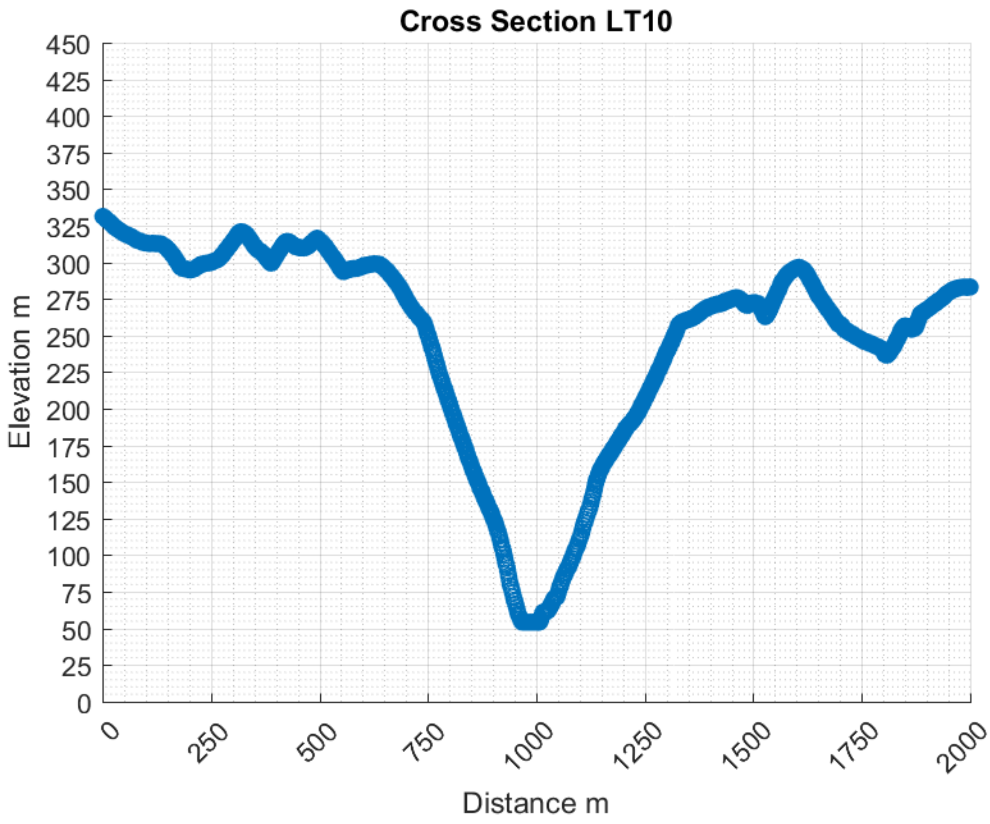

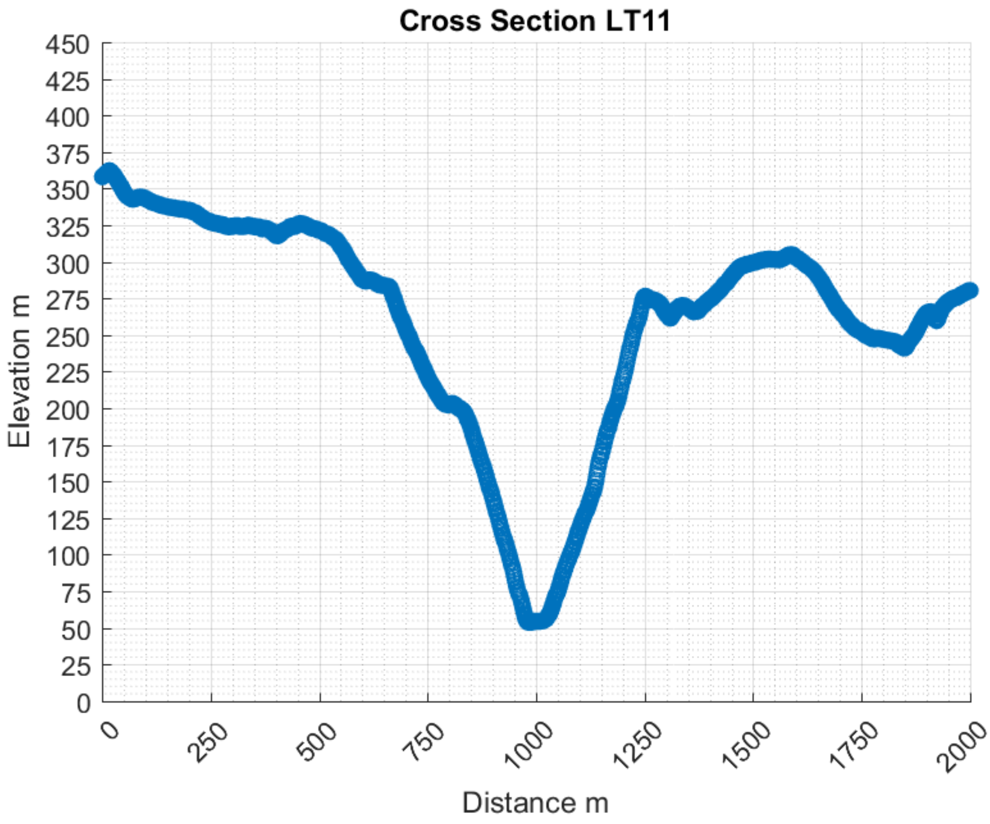
Cross Section LT11
Elevation m
450
425
400
375
350
325
300
275
250
225
200
175
150
125
100
75
50
25
0
0
250
500
750
1000
1250
1500
1750
2000
Distance m

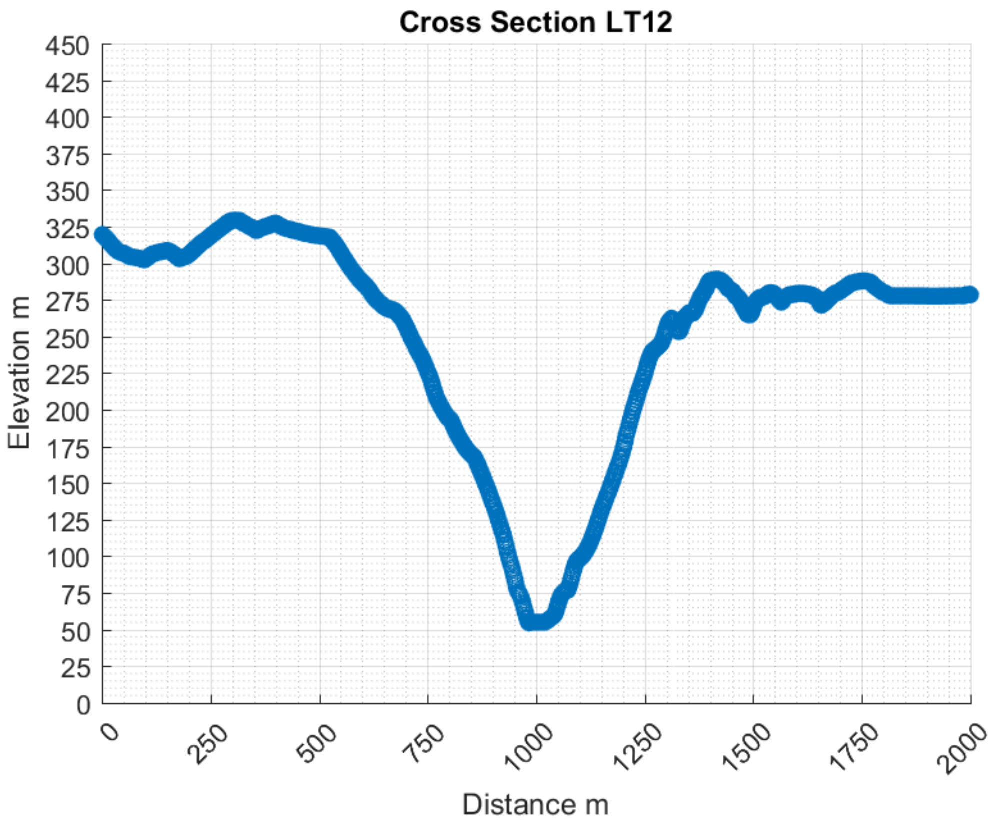
Cross Section LT12
Elevation m
450
425
400
375
350
325
300
275
250
225
200
175
150
125
100
75
50
25
0
0
250
500
750
1000
1250
1500
1750
2000
Distance m

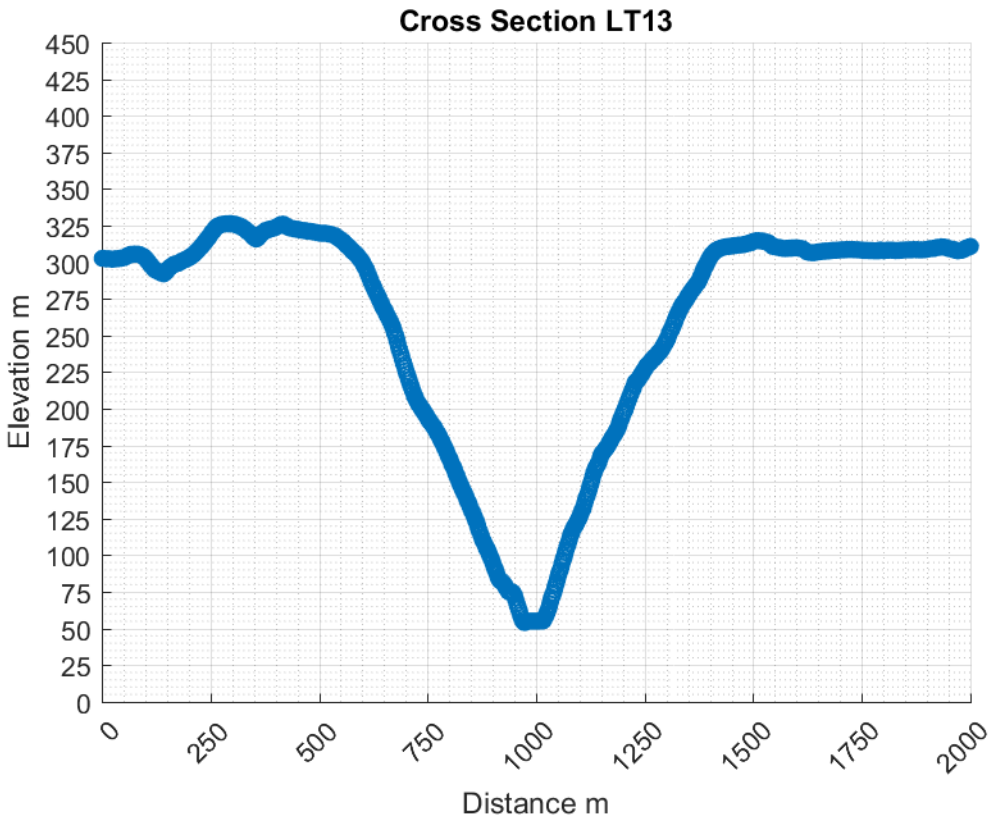

Cross Section LT13
Elevation m
450
425
400
375
350
325
300
275
250
225
200
175
150
125
100
75
50
25
0
0
250
500
750
1000
1250
1500
1750
2000
Distance m

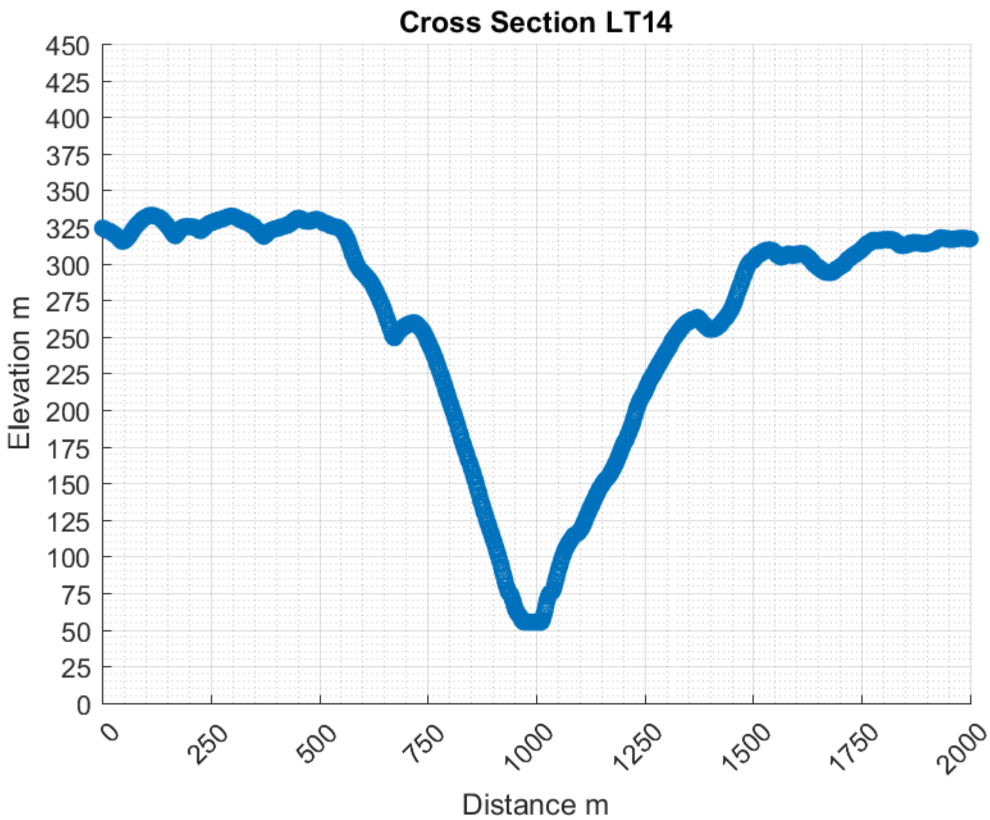

Cross Section LT14
Elevation m
450
425
400
375
350
325
300
275
250
225
200
175
150
125
100
75
50
25
0
0
250
500
750
1000
1250
1500
1750
2000
Distance m

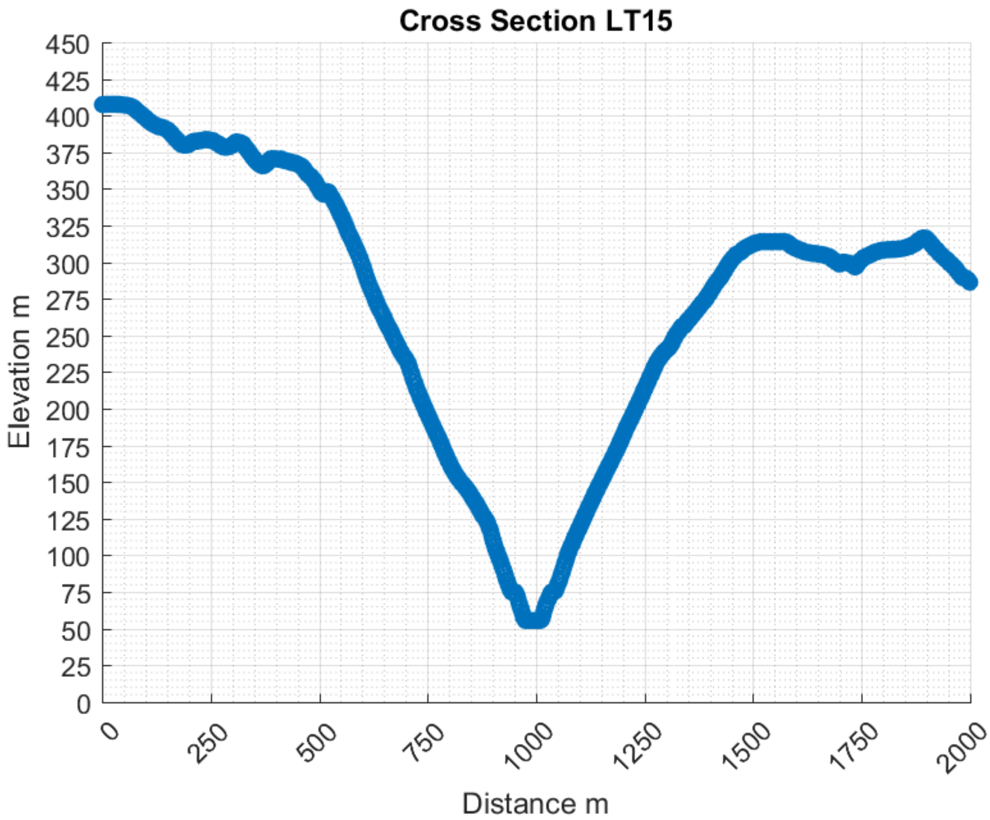
Cross Section LT15
Elevation m
Distance m
450
425
400
375
350
325
300
275
250
225
200
175
150
125
100
75
50
25
0
0
250
500
750
1000
1250
1500
1750
2000

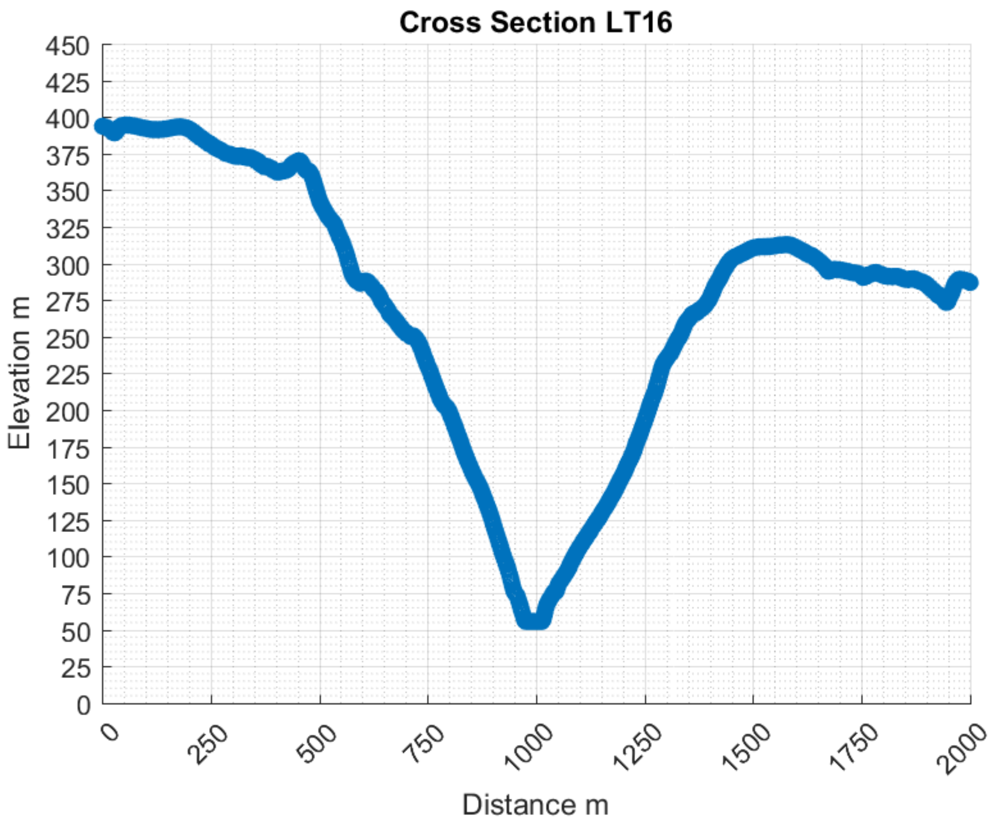
Cross Section LT16
Elevation m
Distance m
450
425
400
375
350
325
300
275
250
225
200
175
150
125
100
75
50
25
0
0
250
500
750
1000
1250
1500
1750
2000

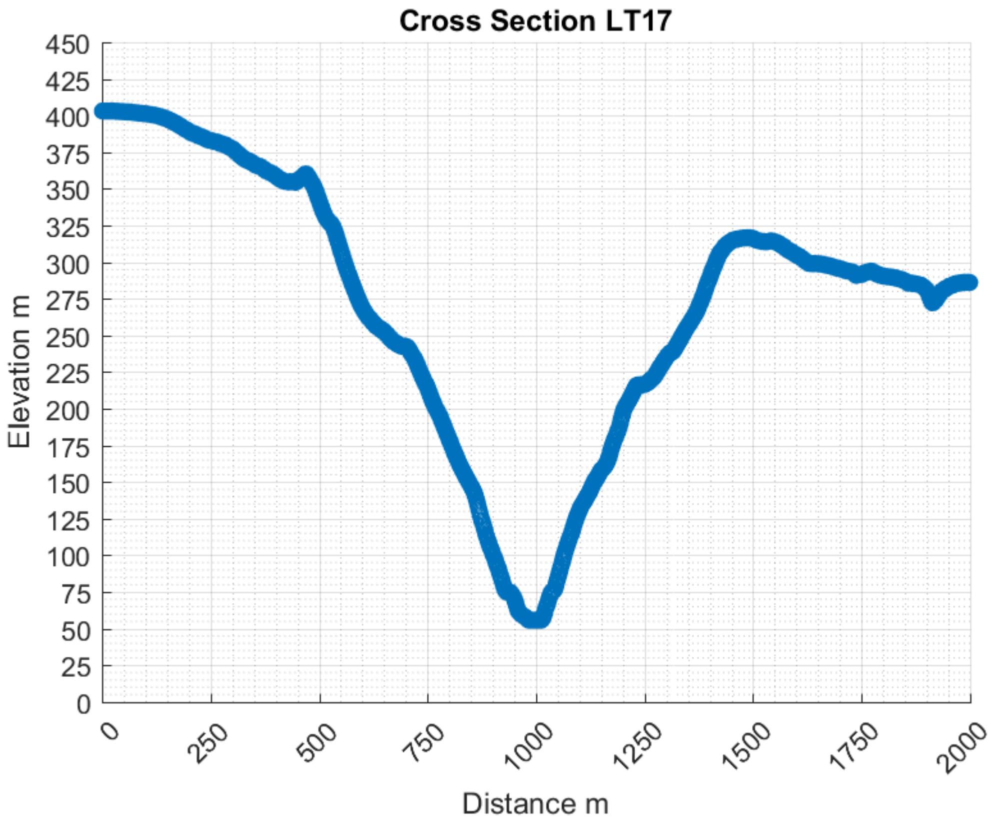
Cross Section LT17
Elevation m
Distance m
0
25
50
75
100
125
150
175
200
225
250
275
300
325
350
375
400
425
450
0
250
500
750
1000
1250
1500
1750
2000

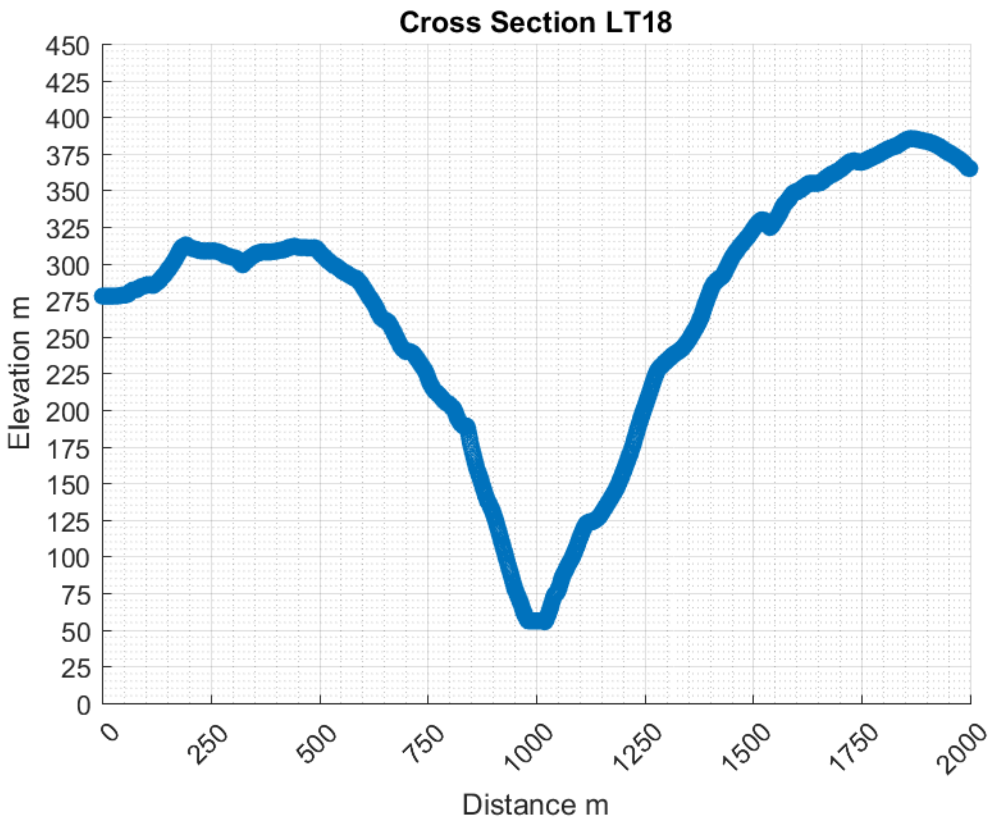
Cross Section LT18
Elevation m
Distance m
0
25
50
75
100
125
150
175
200
225
250
275
300
325
350
375
400
425
450
0
250
500
750
1000
1250
1500
1750
2000

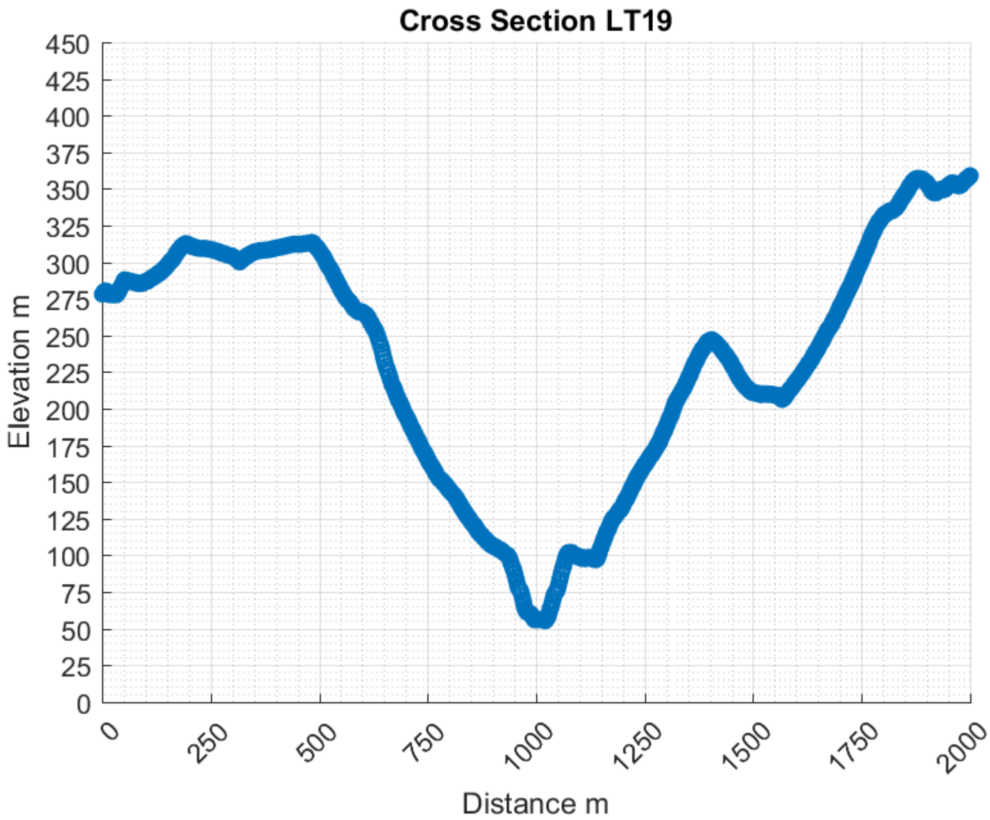
Cross Section LT19
Elevation m
450
425
400
375
350
325
300
275
250
225
200
175
150
125
100
75
50
25
0
0
250
500
750
1000
1250
1500
1750
2000
Distance m

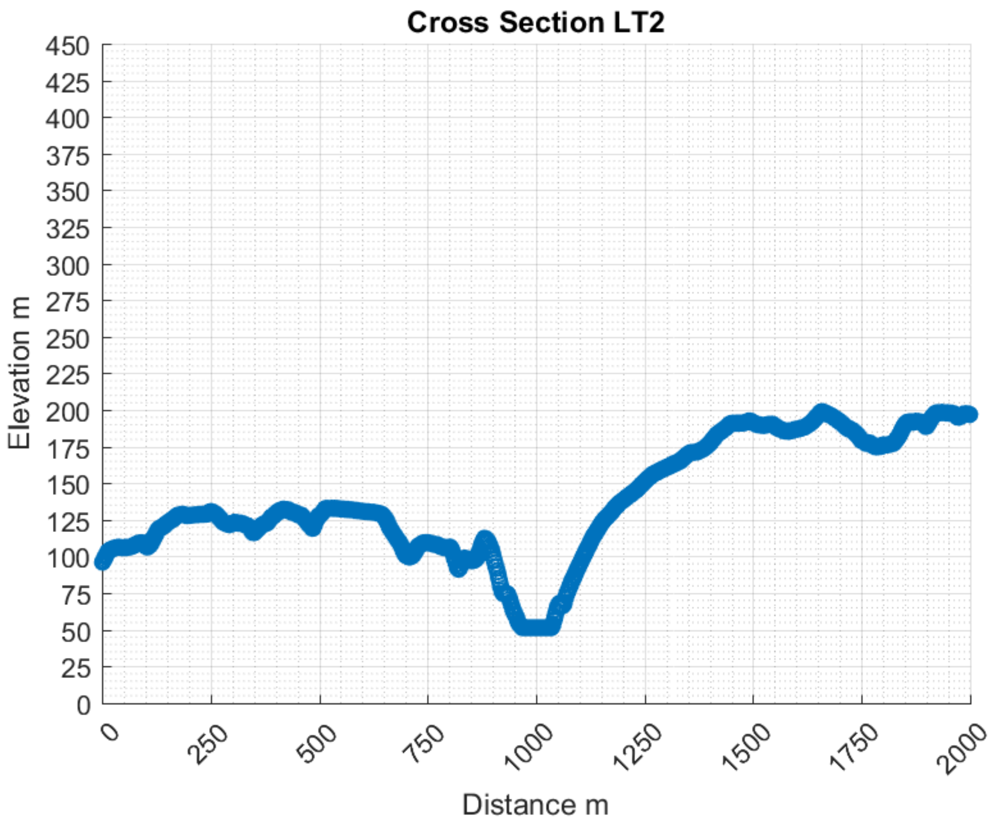
Cross Section LT2
Elevation m
450
425
400
375
350
325
300
275
250
225
200
175
150
125
100
75
50
25
0
0
250
500
750
1000
1250
1500
1750
2000
Distance m

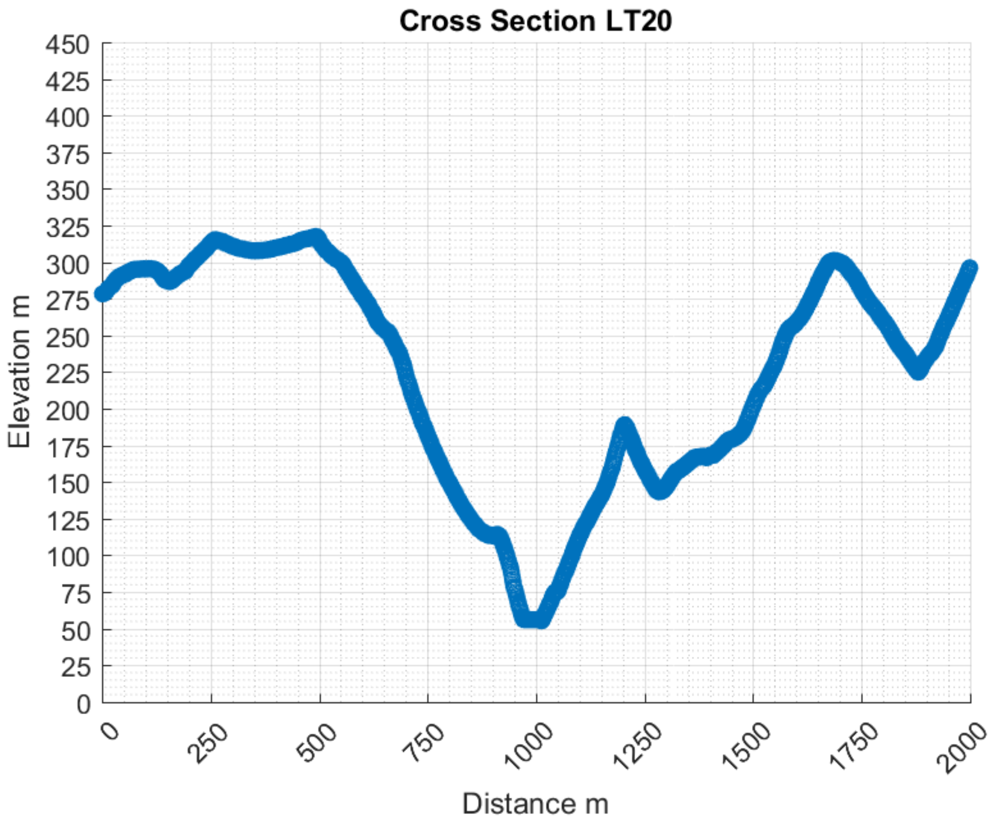
Cross Section LT20
Elevation m
Distance m
450
425
400
375
350
325
300
275
250
225
200
175
150
125
100
75
50
25
0
0
250
500
750
1000
1250
1500
1750
2000

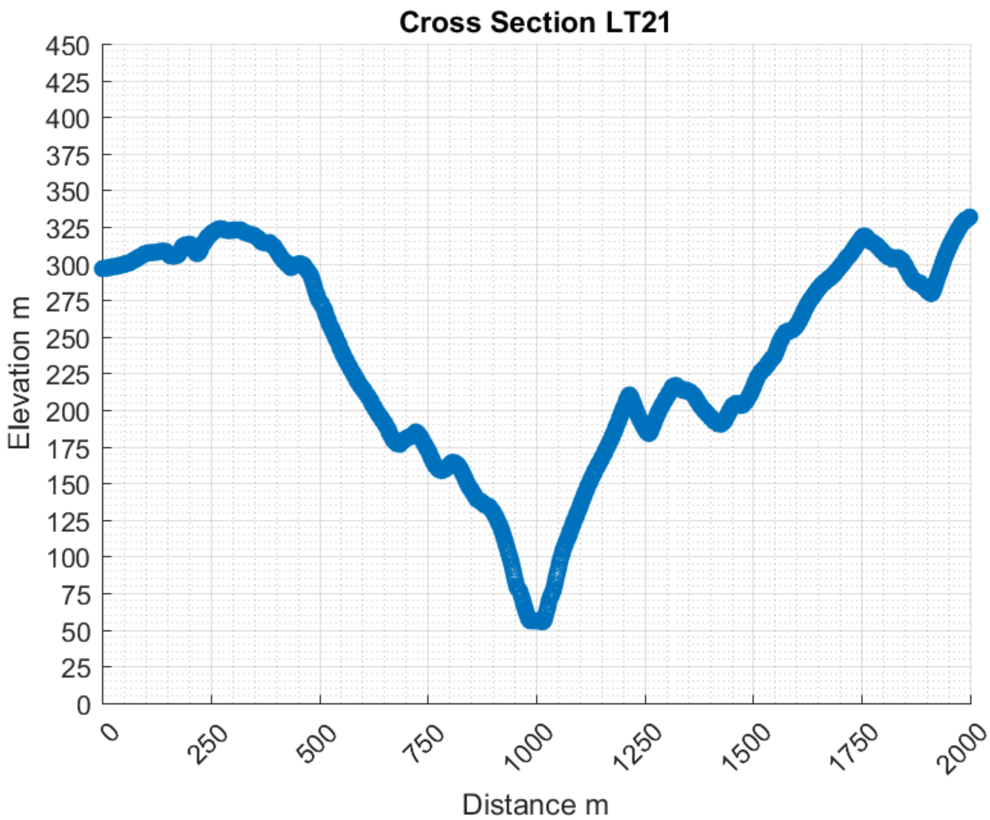
Cross Section LT21
Elevation m
Distance m
450
425
400
375
350
325
300
275
250
225
200
175
150
125
100
75
50
25
0
0
250
500
750
1000
1250
1500
1750
2000

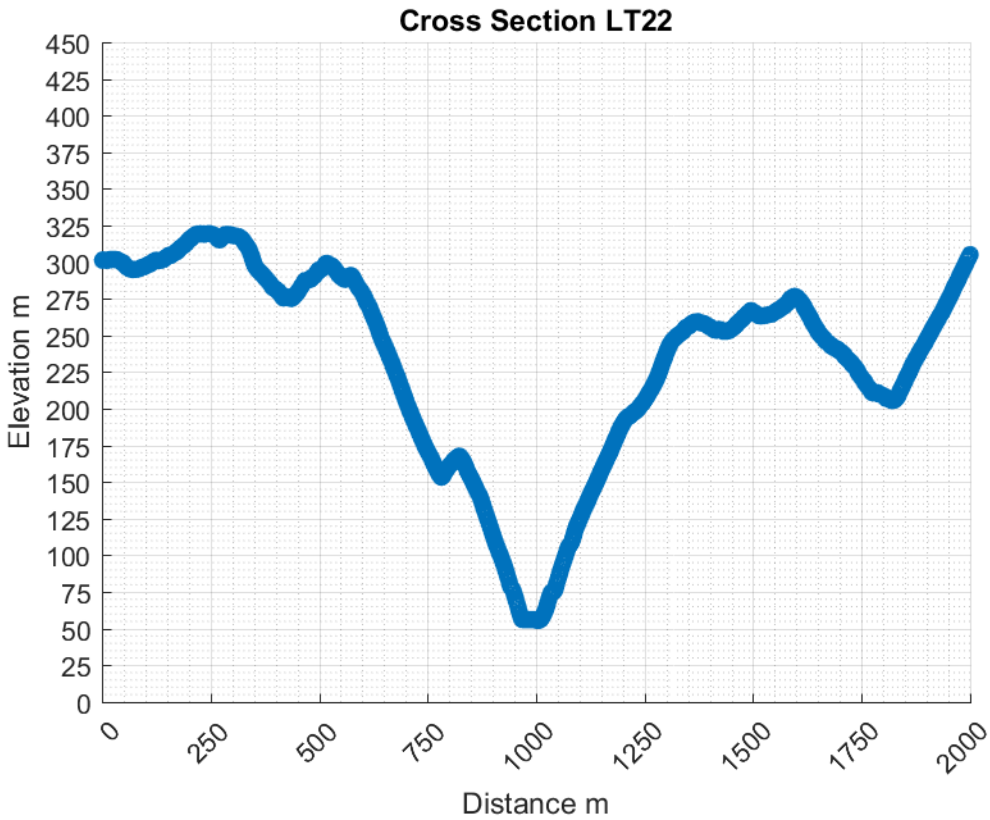
Cross Section LT22
Elevation m
450
425
400
375
350
325
300
275
250
225
200
175
150
125
100
75
50
25
0
0
250
500
750
1000
1250
1500
1750
2000
Distance m

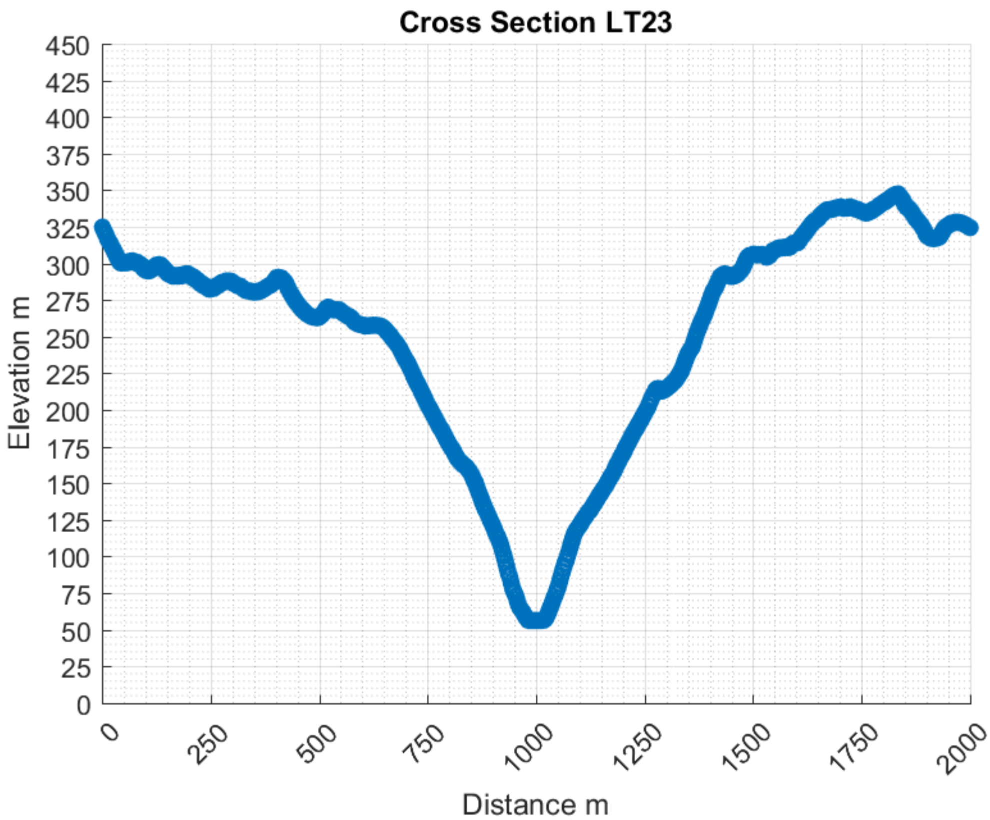
Cross Section LT23
Elevation m
450
425
400
375
350
325
300
275
250
225
200
175
150
125
100
75
50
25
0
0
250
500
750
1000
1250
1500
1750
2000
Distance m

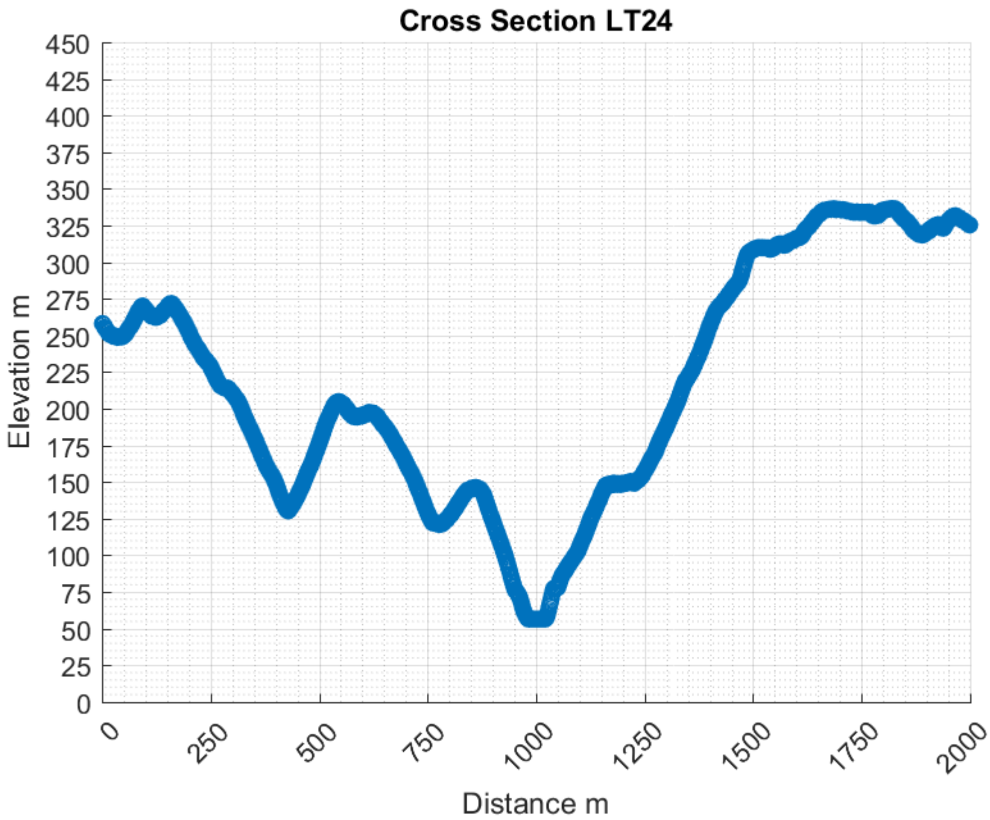
Cross Section LT24
Elevation m
450
425
400
375
350
325
300
275
250
225
200
175
150
125
100
75
50
25
0
0
250
500
750
1000
1250
1500
1750
2000
Distance m

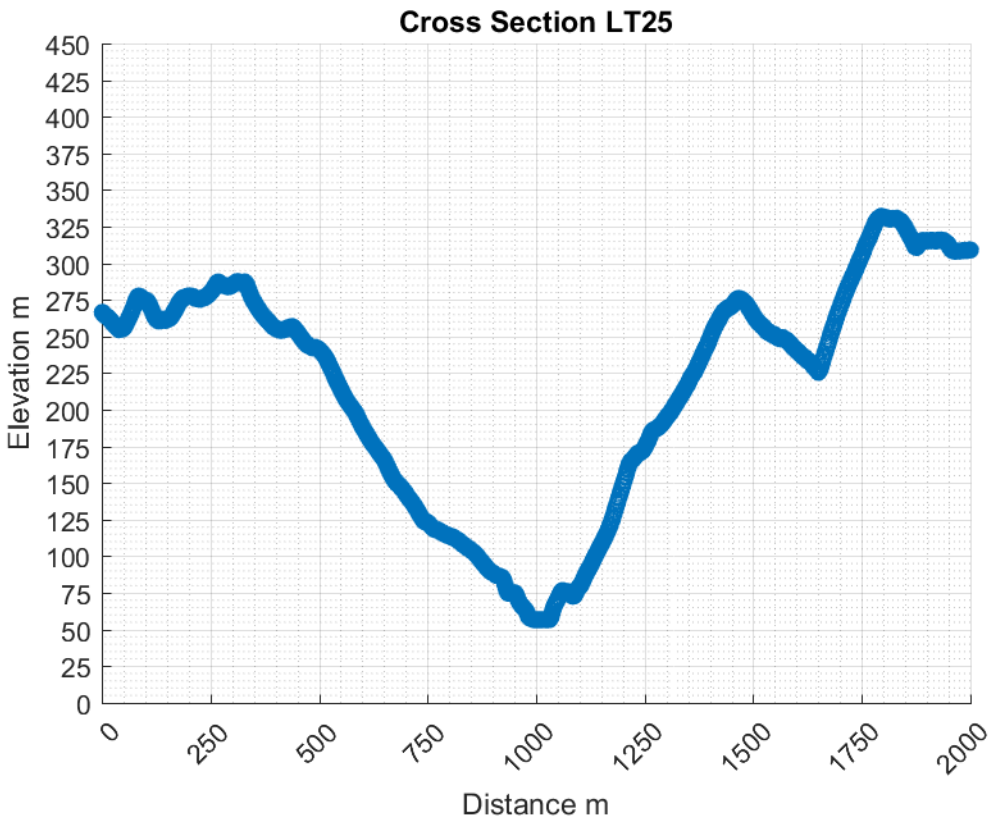
Cross Section LT25
Elevation m
450
425
400
375
350
325
300
275
250
225
200
175
150
125
100
75
50
25
0
0
250
500
750
1000
1250
1500
1750
2000
Distance m

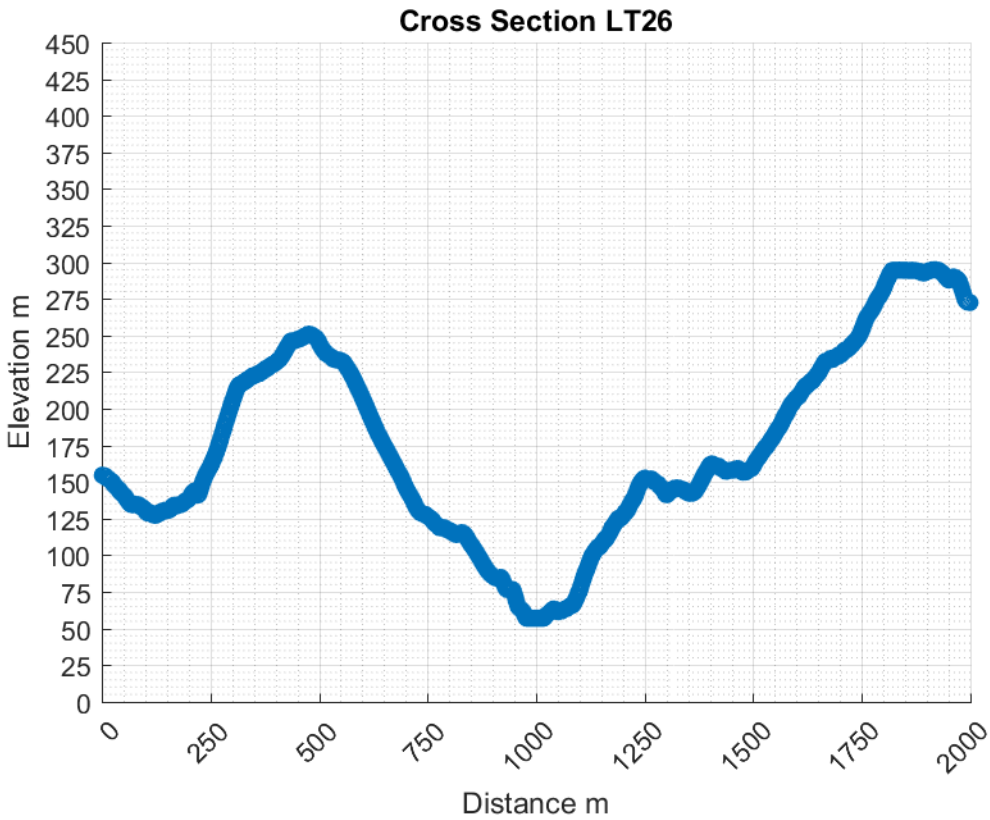
Cross Section LT26
Elevation m
Distance m
450
425
400
375
350
325
300
275
250
225
200
175
150
125
100
75
50
25
0
0
250
500
750
1000
1250
1500
1750
2000

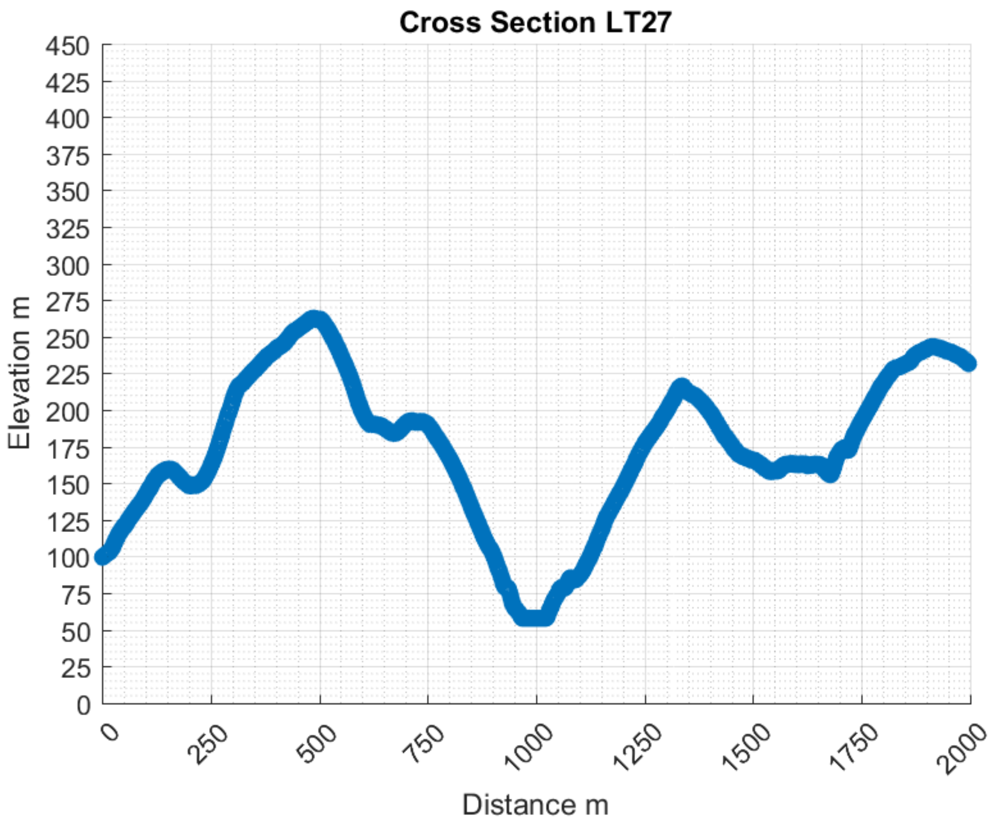
Cross Section LT27
Elevation m
Distance m
450
425
400
375
350
325
300
275
250
225
200
175
150
125
100
75
50
25
0
0
250
500
750
1000
1250
1500
1750
2000

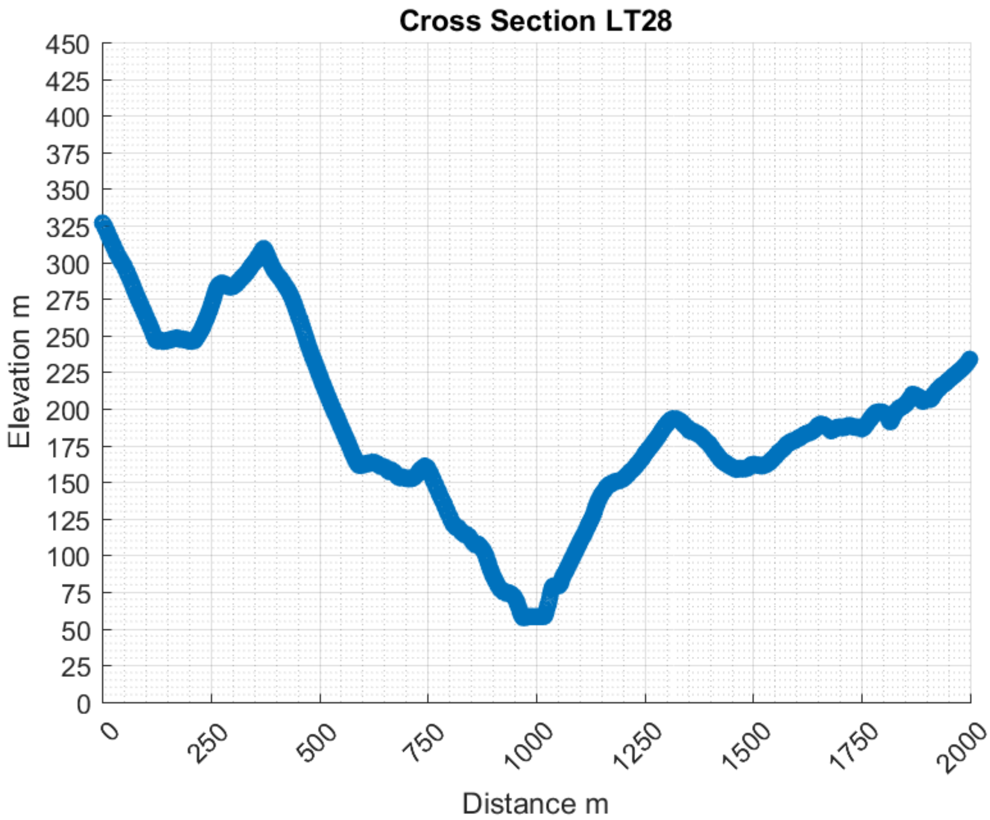
Cross Section LT28
Elevation m
450
425
400
375
350
325
300
275
250
225
200
175
150
125
100
75
50
25
0
250
500
750
1000
1250
1500
1750
2000
Distance m

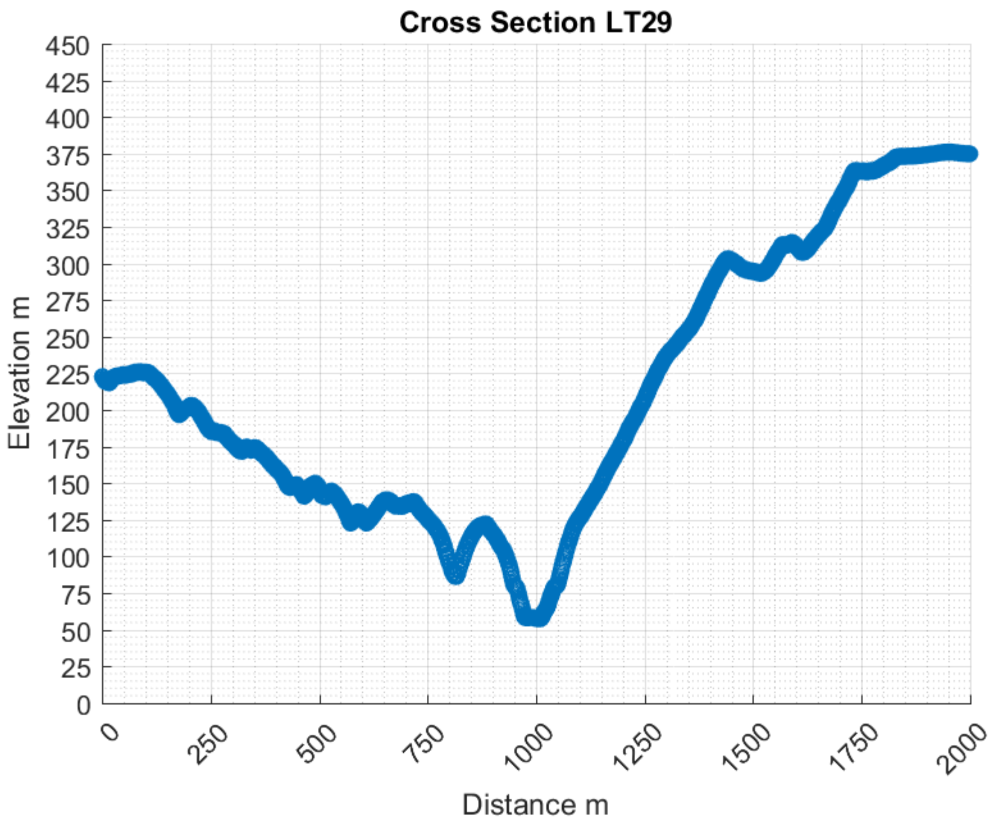
Cross Section LT29
Elevation m
450
425
400
375
350
325
300
275
250
225
200
175
150
125
100
75
50
25
0
250
500
750
1000
1250
1500
1750
2000
Distance m

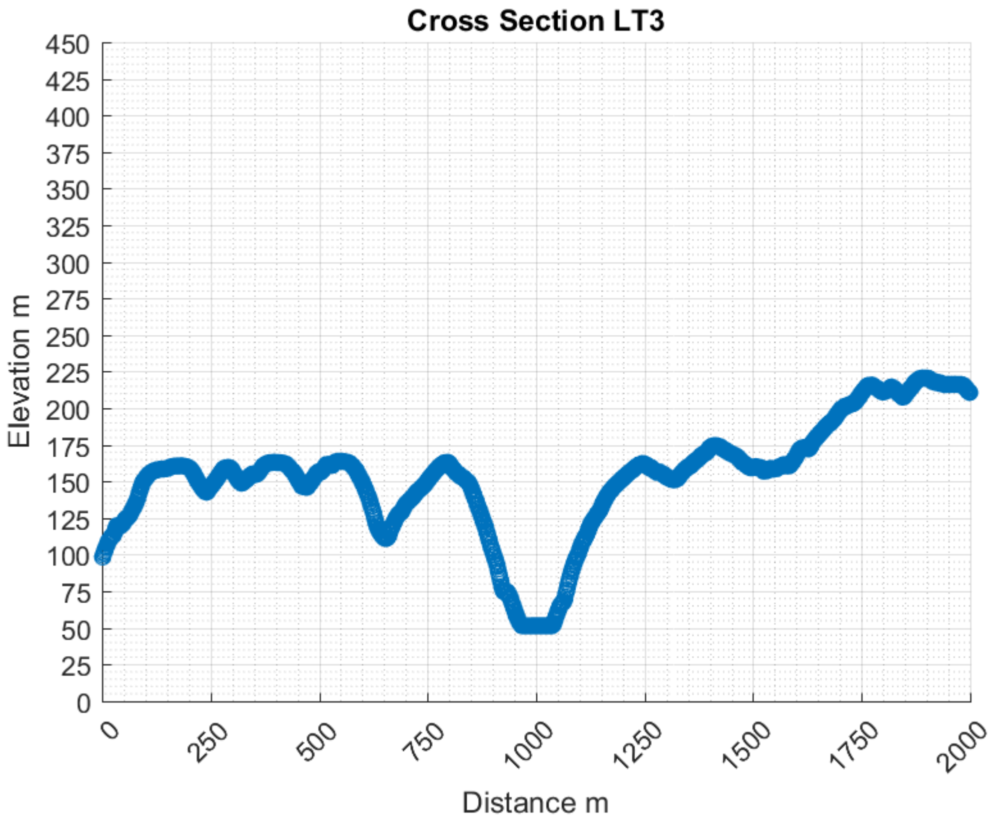
Cross Section LT3
Elevation m
450
425
400
375
350
325
300
275
250
225
200
175
150
125
100
75
50
25
0
0
250
500
750
1000
1250
1500
1750
2000
Distance m

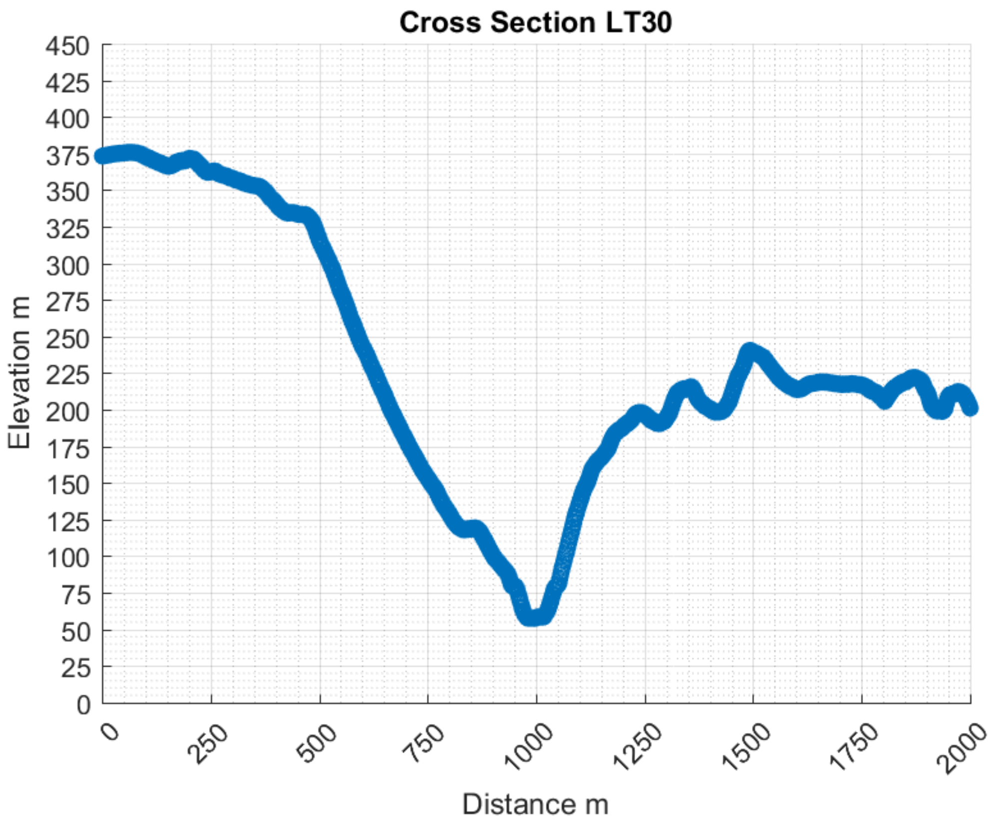
Cross Section LT30
Elevation m
450
425
400
375
350
325
300
275
250
225
200
175
150
125
100
75
50
25
0
0
250
500
750
1000
1250
1500
1750
2000
Distance m

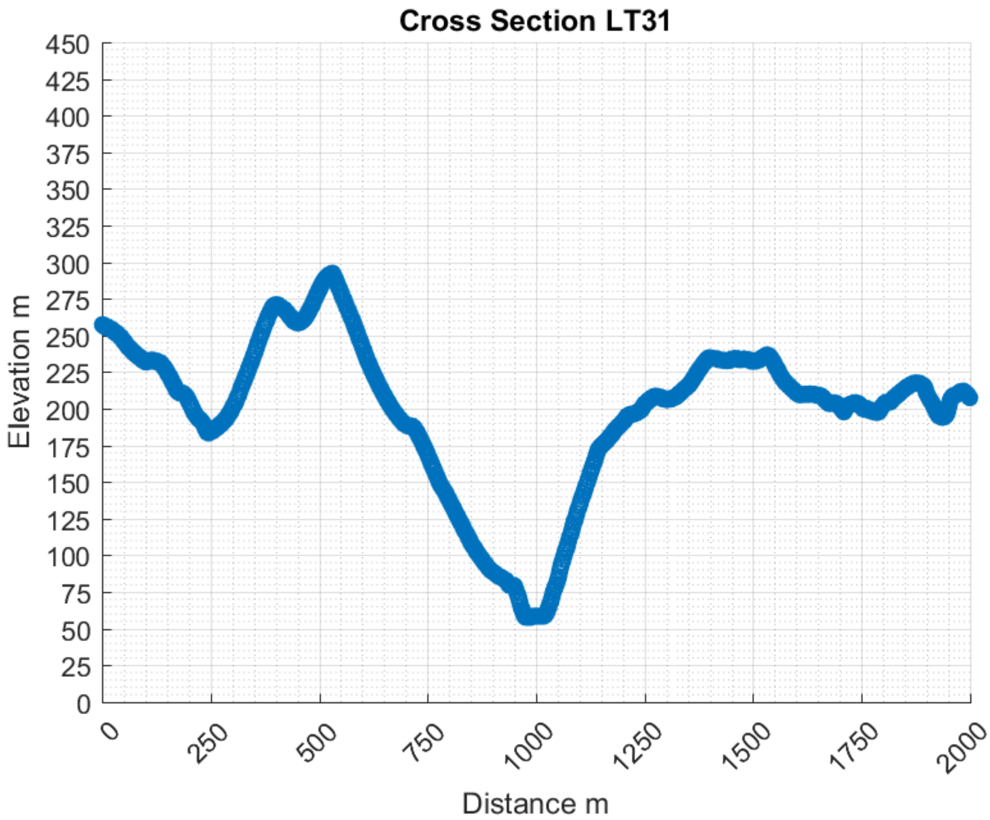
Cross Section LT31
Elevation m
450
425
400
375
350
325
300
275
250
225
200
175
150
125
100
75
50
25
0
0
250
500
750
1000
1250
1500
1750
2000
Distance m

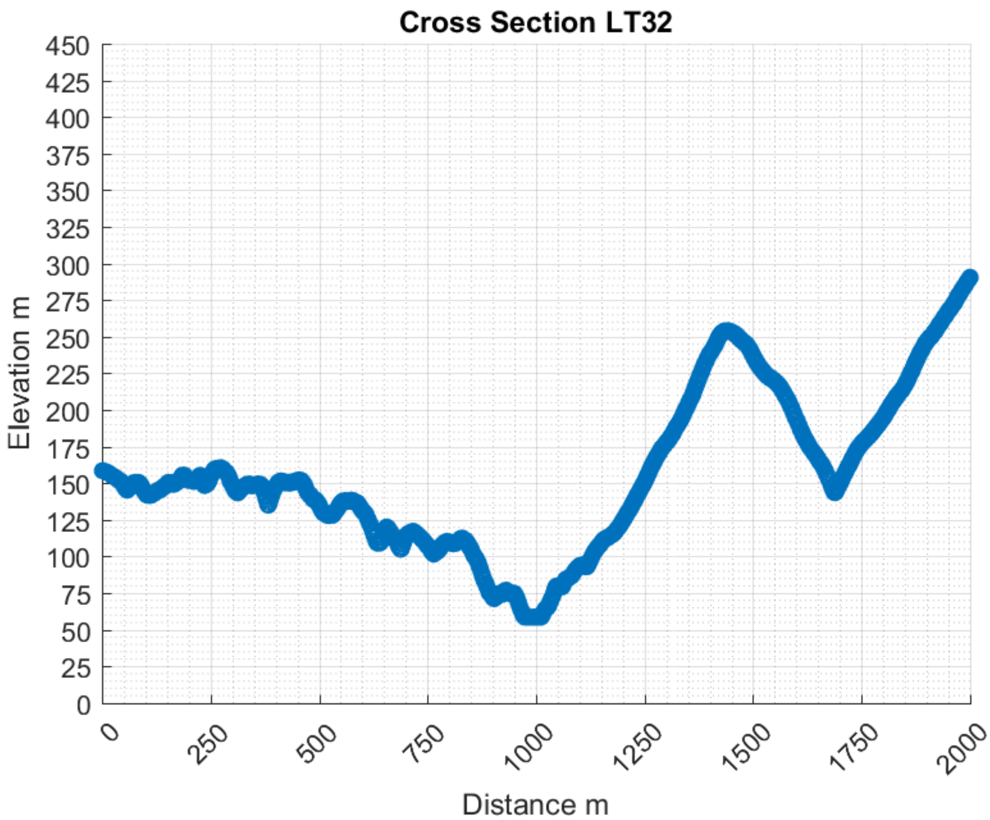
Cross Section LT32
Elevation m
450
425
400
375
350
325
300
275
250
225
200
175
150
125
100
75
50
25
0
0
250
500
750
1000
1250
1500
1750
2000
Distance m

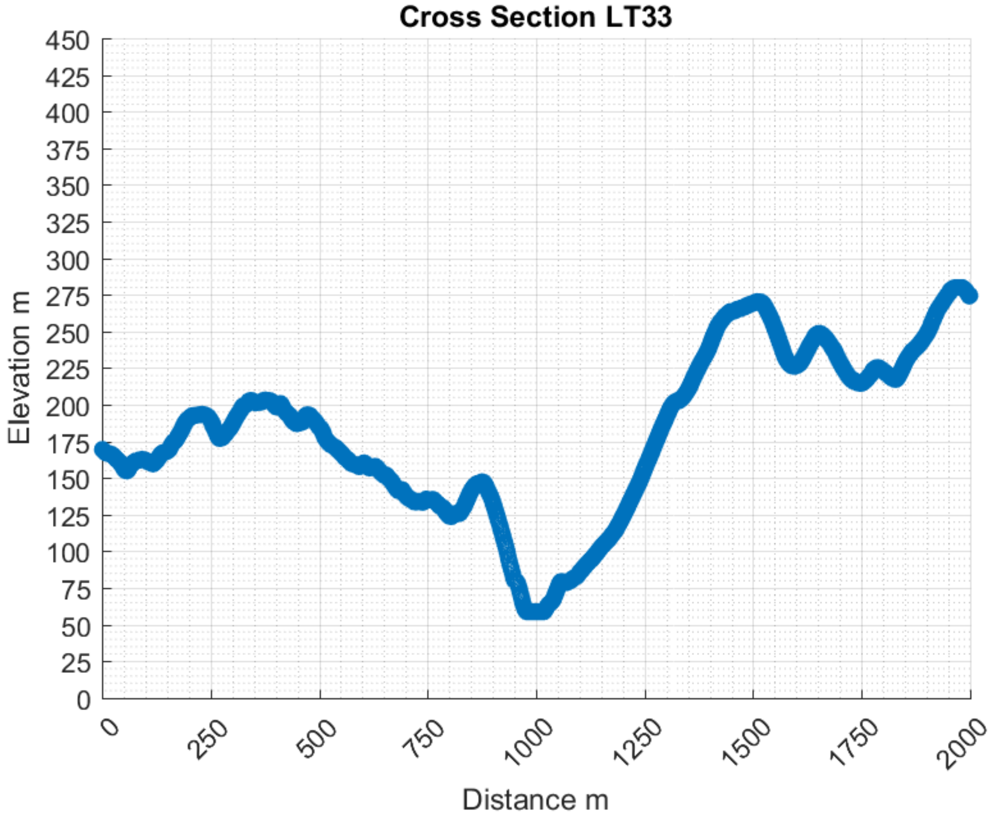
Cross Section LT33
Elevation m
Distance m
0
25
50
75
100
125
150
175
200
225
250
275
300
325
350
375
400
425
450
0
250
500
750
1000
1250
1500
1750
2000

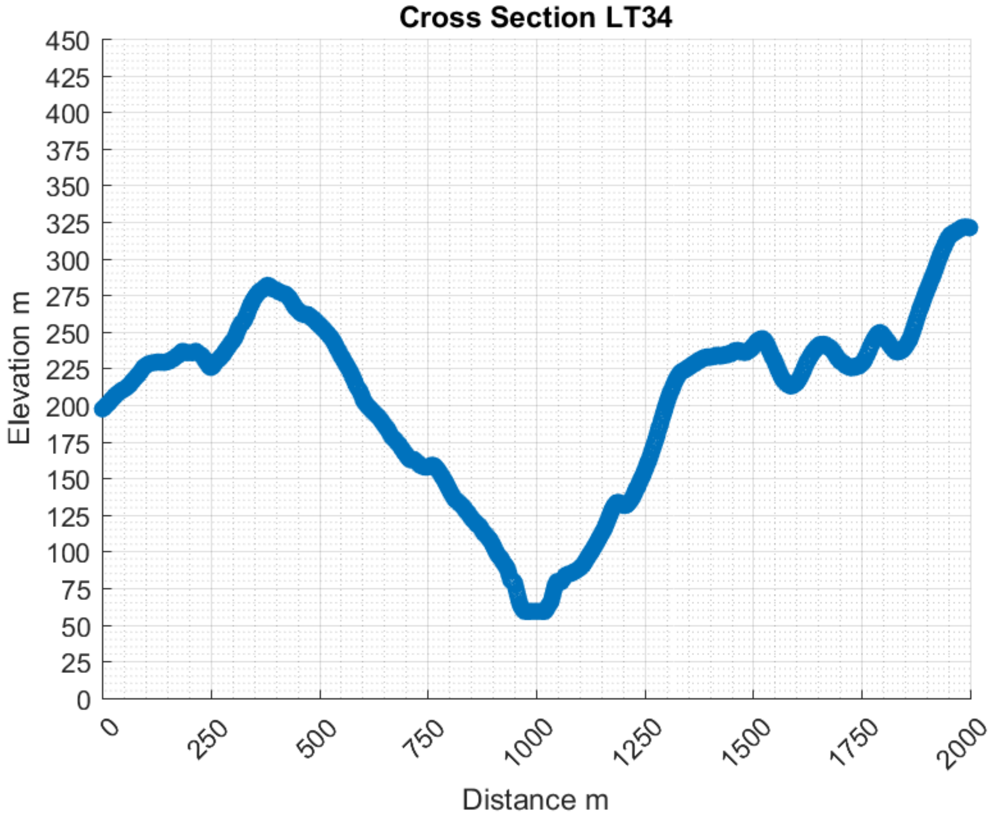
Cross Section LT34
Elevation m
Distance m
0
25
50
75
100
125
150
175
200
225
250
275
300
325
350
375
400
425
450
0
250
500
750
1000
1250
1500
1750
2000

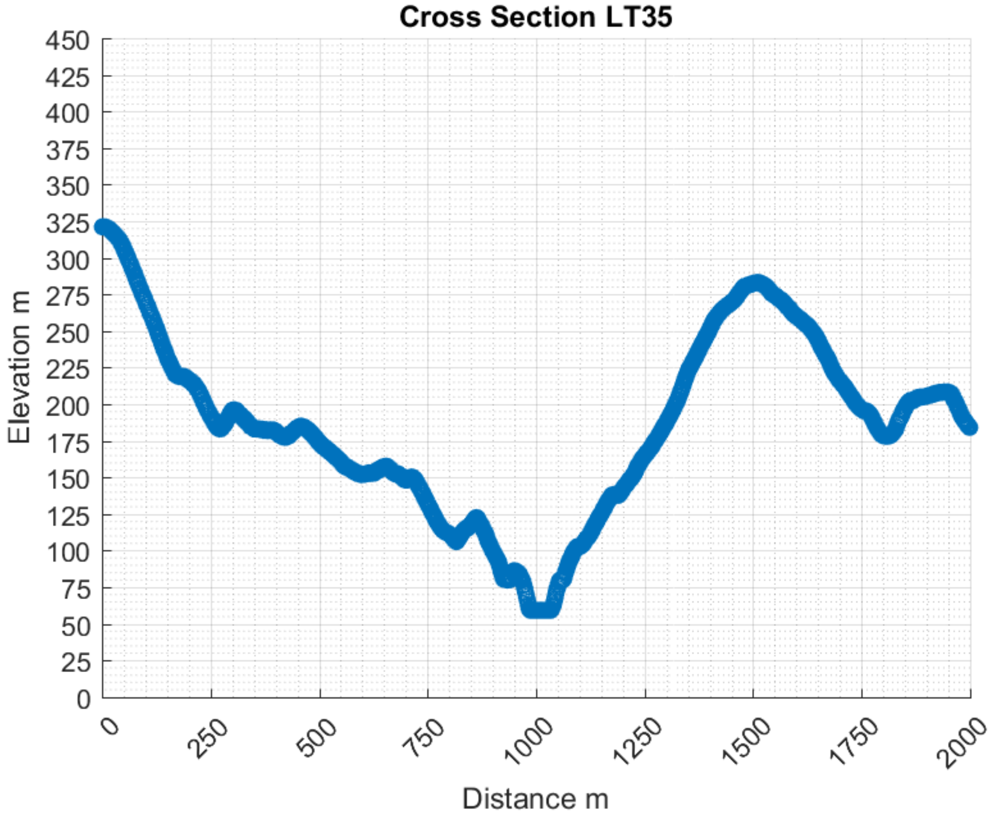
Cross Section LT35
Elevation m
450
425
400
375
350
325
300
275
250
225
200
175
150
125
100
75
50
25
0
0
250
500
750
1000
1250
1500
1750
2000
Distance m

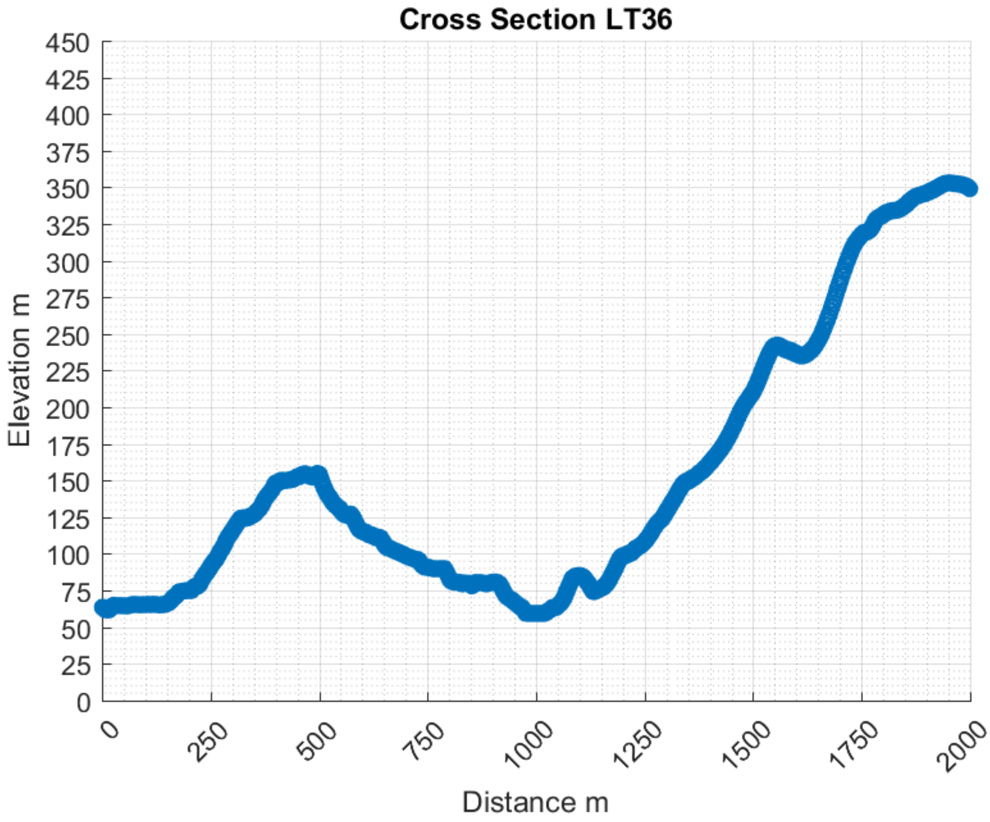
Cross Section LT36
Elevation m
450
425
400
375
350
325
300
275
250
225
200
175
150
125
100
75
50
25
0
0
250
500
750
1000
1250
1500
1750
2000
Distance m

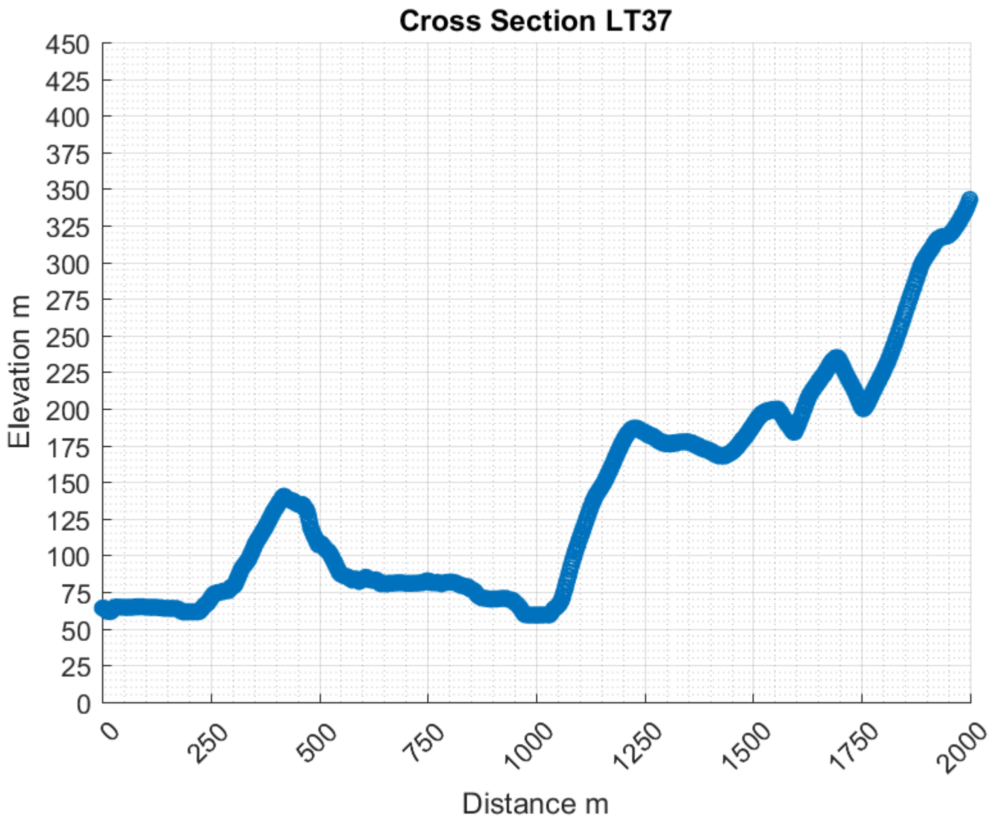
Cross Section LT37
Elevation m
Distance m
0
25
50
75
100
125
150
175
200
225
250
275
300
325
350
375
400
425
450
0
250
500
750
1000
1250
1500
1750
2000

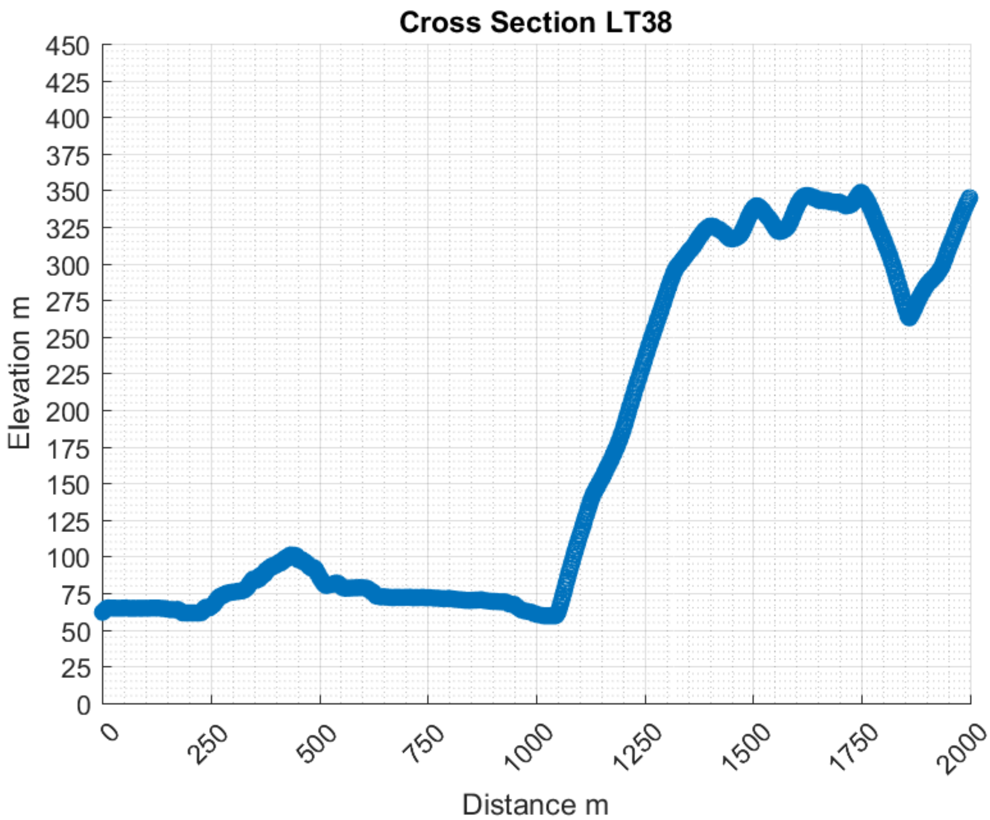
Cross Section LT38
Elevation m
Distance m
0
25
50
75
100
125
150
175
200
225
250
275
300
325
350
375
400
425
450
0
250
500
750
1000
1250
1500
1750
2000

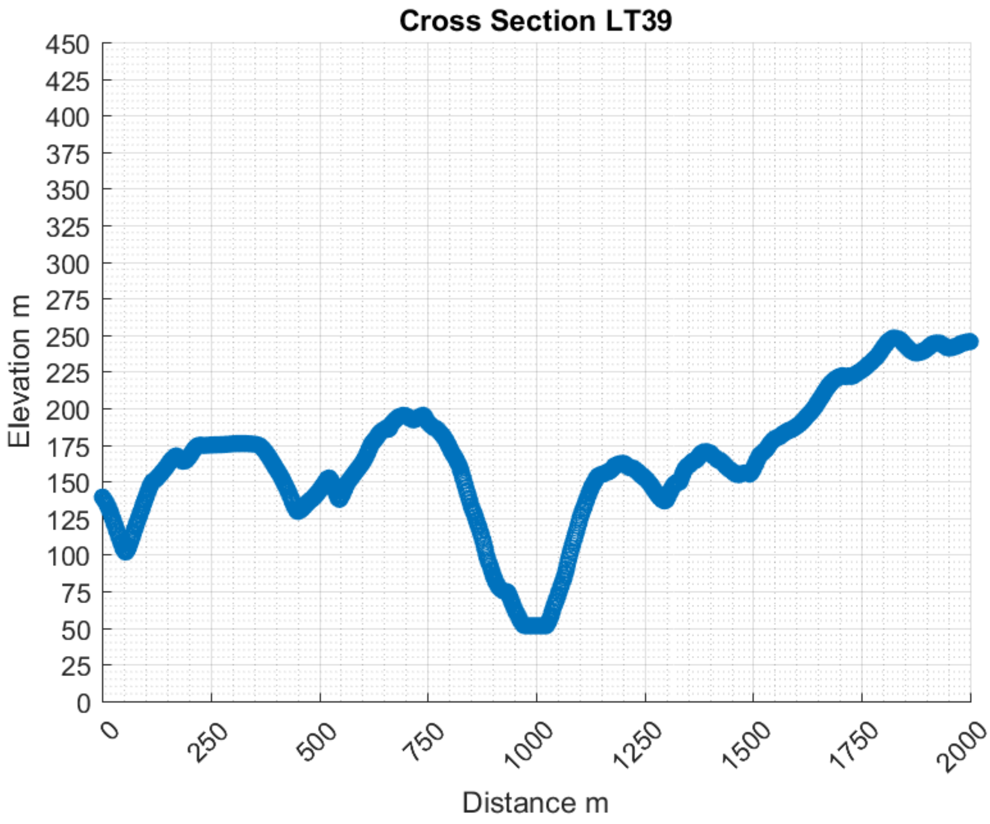

Cross Section LT39
Elevation m
Distance m
0
25
50
75
100
125
150
175
200
225
250
275
300
325
350
375
400
425
450
0
250
500
750
1000
1250
1500
1750
2000

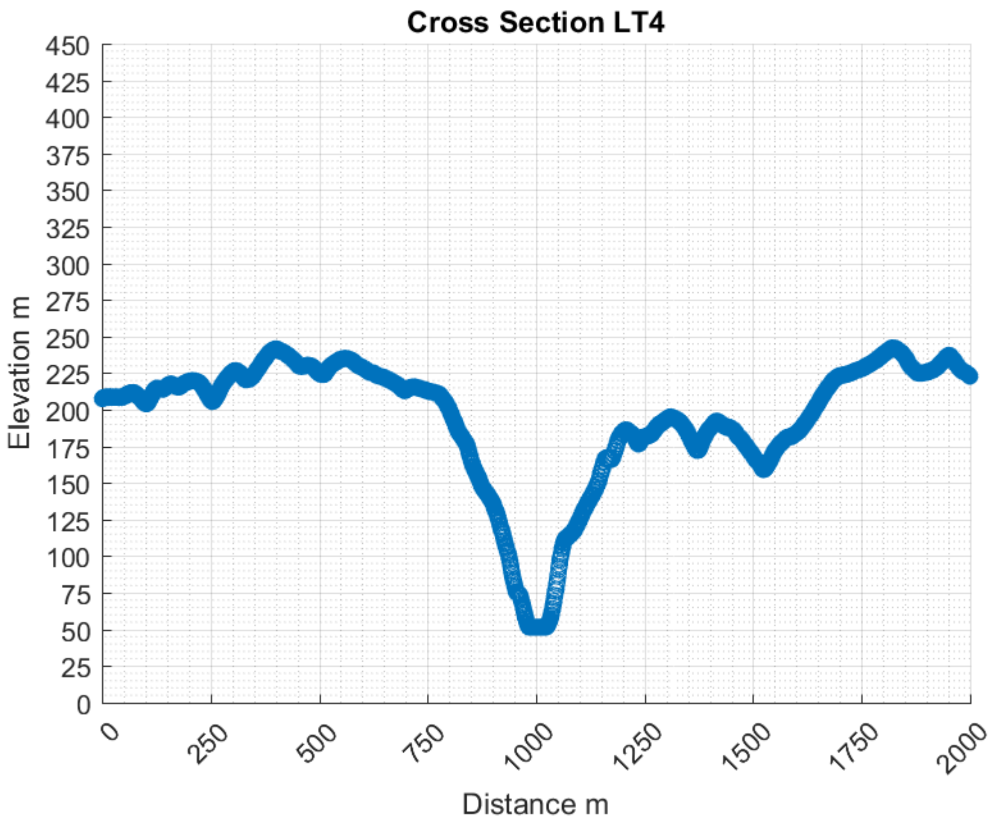

Cross Section LT4
Elevation m
Distance m
0
25
50
75
100
125
150
175
200
225
250
275
300
325
350
375
400
425
450
0
250
500
750
1000
1250
1500
1750
2000

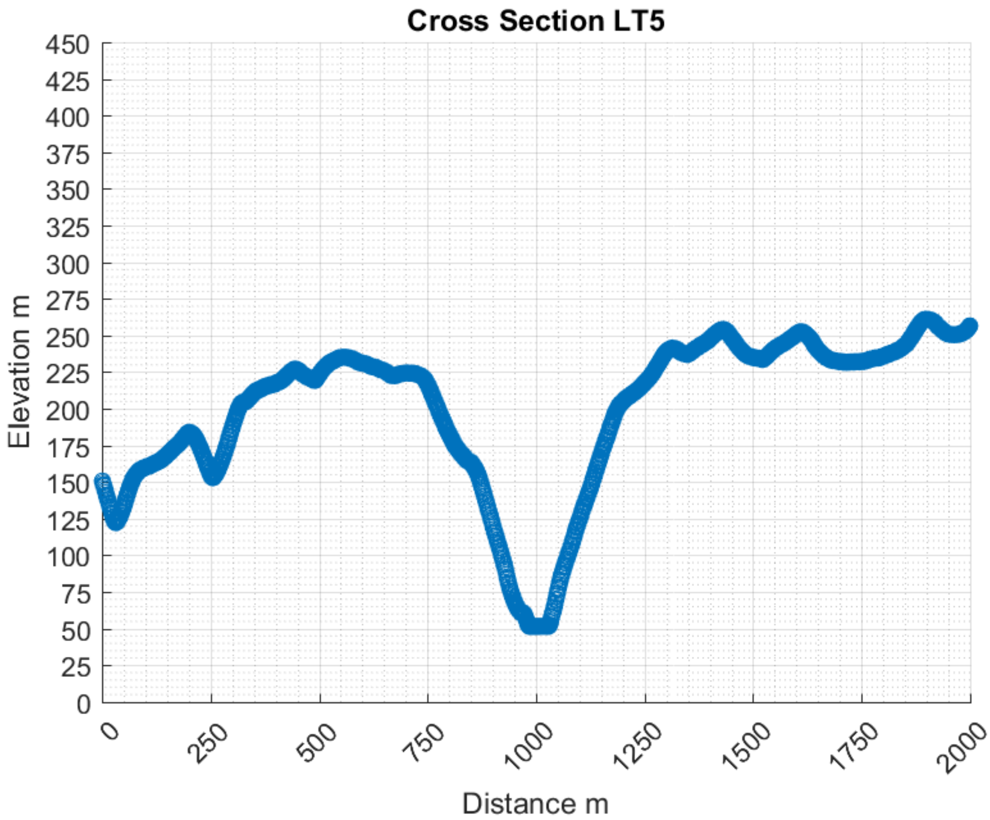
Cross Section LT5
Elevation m
450
425
400
375
350
325
300
275
250
225
200
175
150
125
100
75
50
25
0
0
250
500
750
1000
1250
1500
1750
2000
Distance m

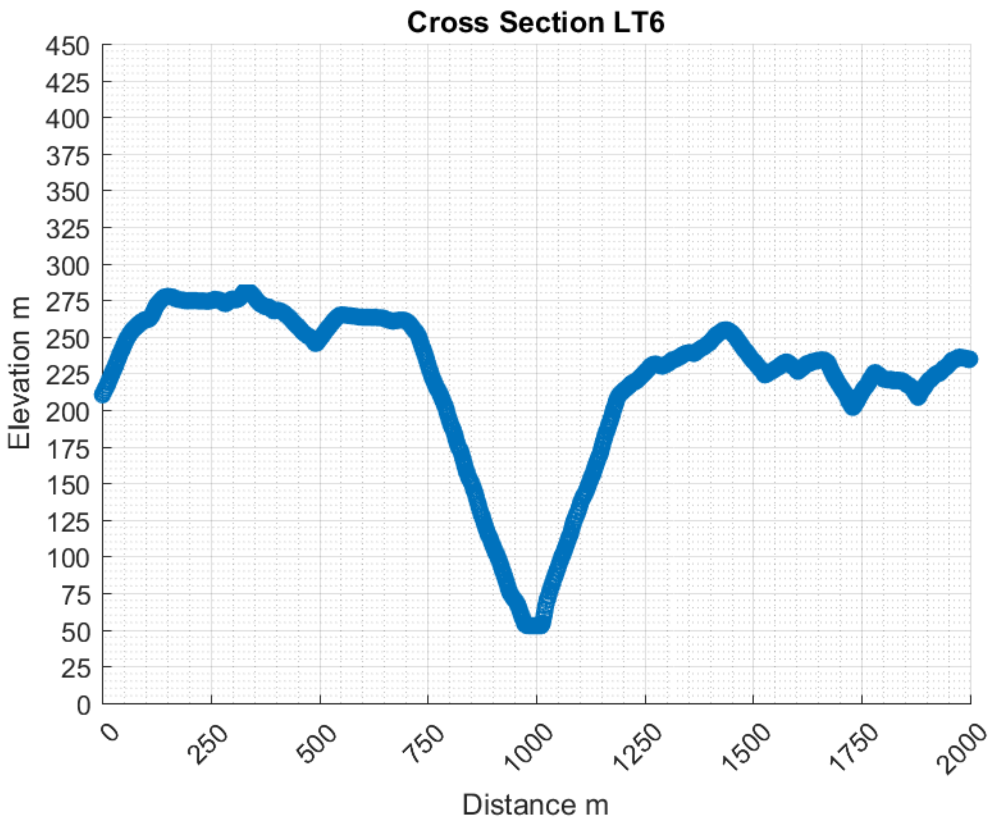
Cross Section LT6
Elevation m
450
425
400
375
350
325
300
275
250
225
200
175
150
125
100
75
50
25
0
0
250
500
750
1000
1250
1500
1750
2000
Distance m

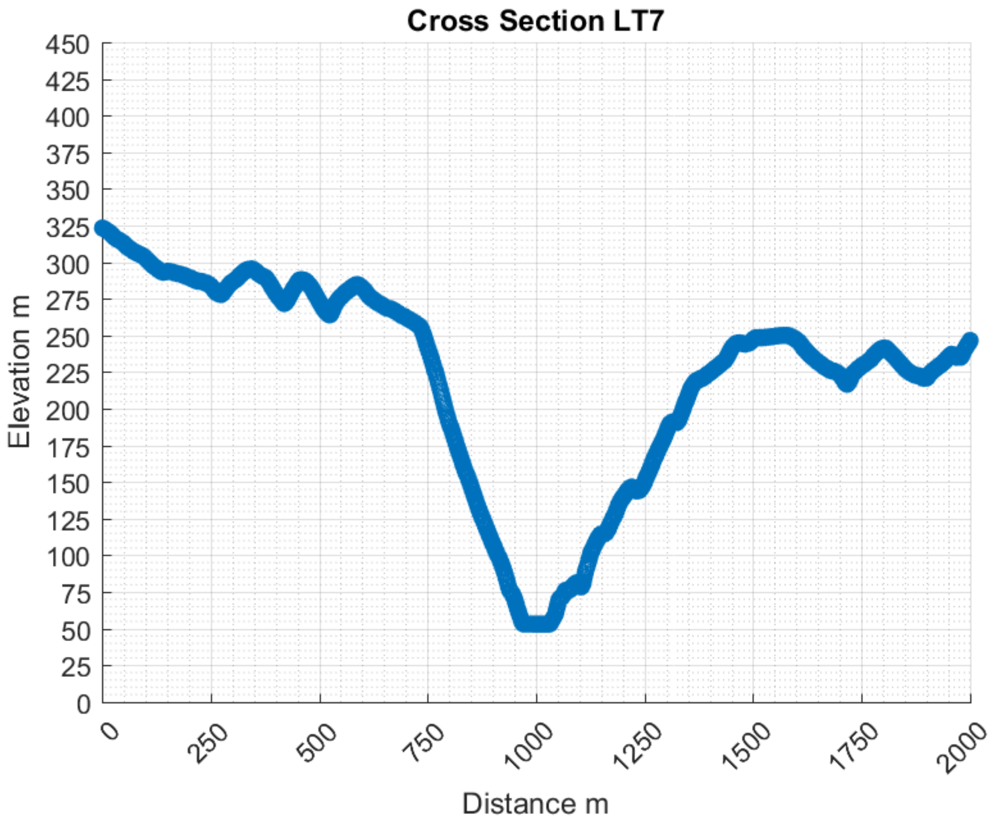
Cross Section LT7
Elevation m
450
425
400
375
350
325
300
275
250
225
200
175
150
125
100
75
50
25
0
0
250
500
750
1000
1250
1500
1750
2000
Distance m

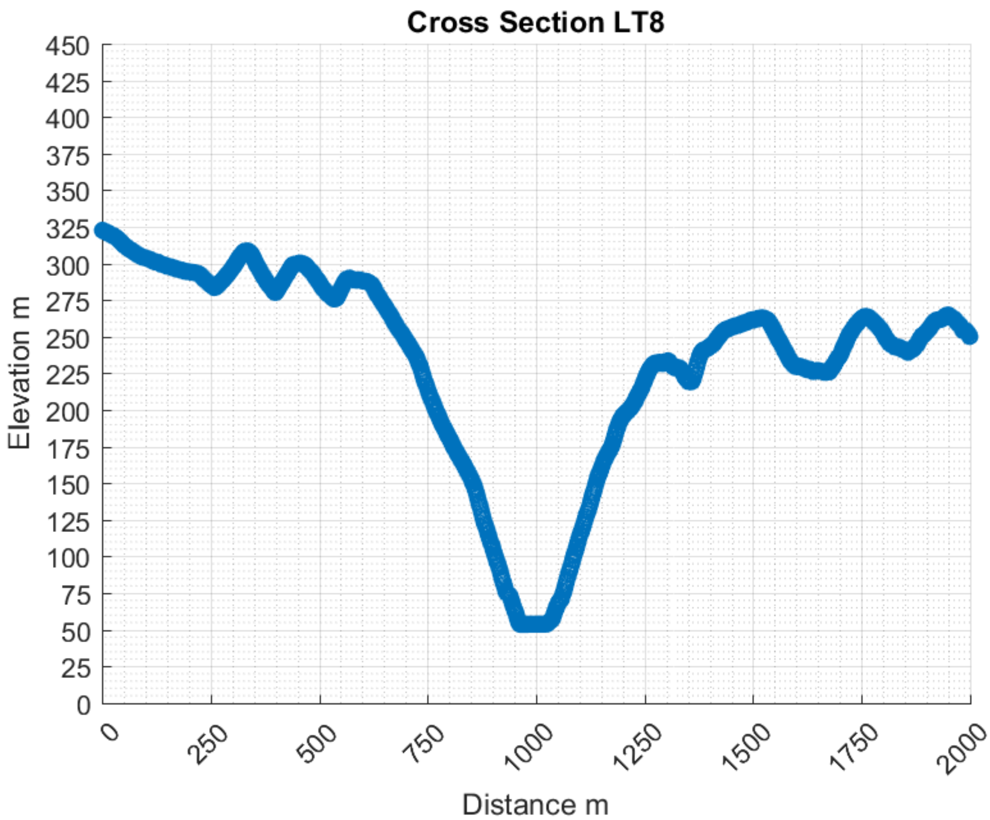
Cross Section LT8
Elevation m
450
425
400
375
350
325
300
275
250
225
200
175
150
125
100
75
50
25
0
0
250
500
750
1000
1250
1500
1750
2000
Distance m

APPENDIX 2 LANDSLIDE SIMULATION CROSS-SECTIONS

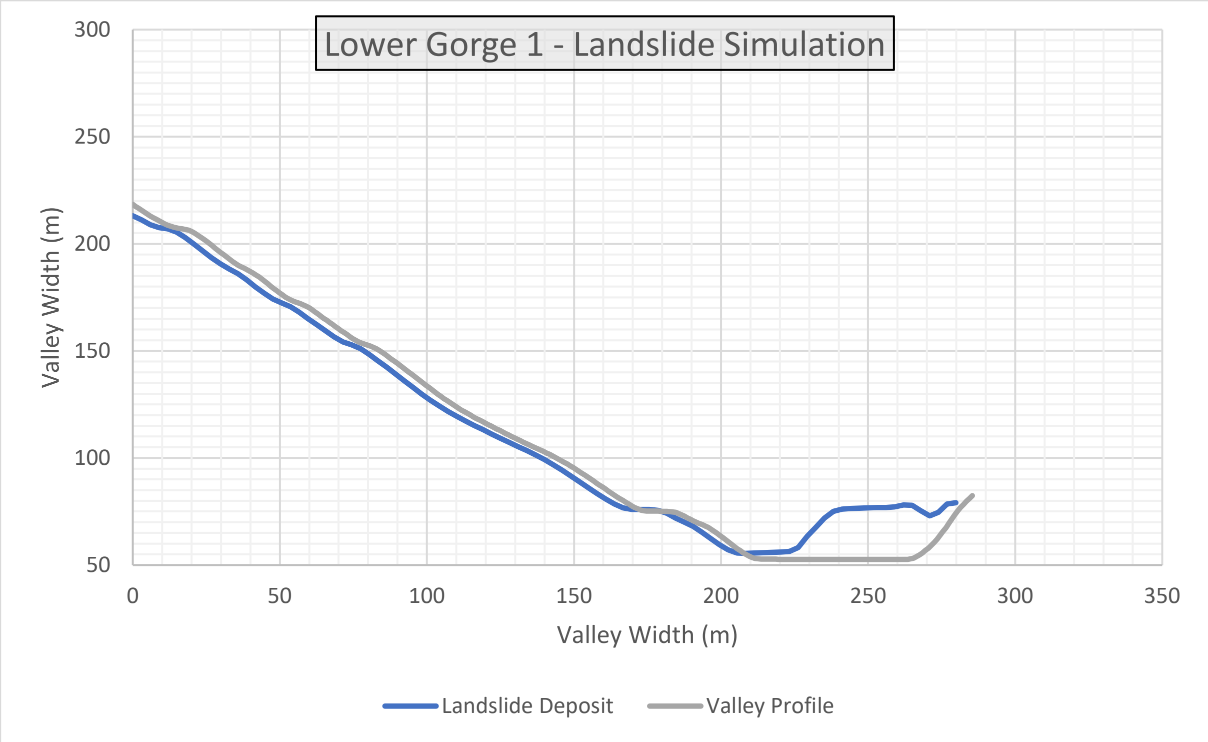

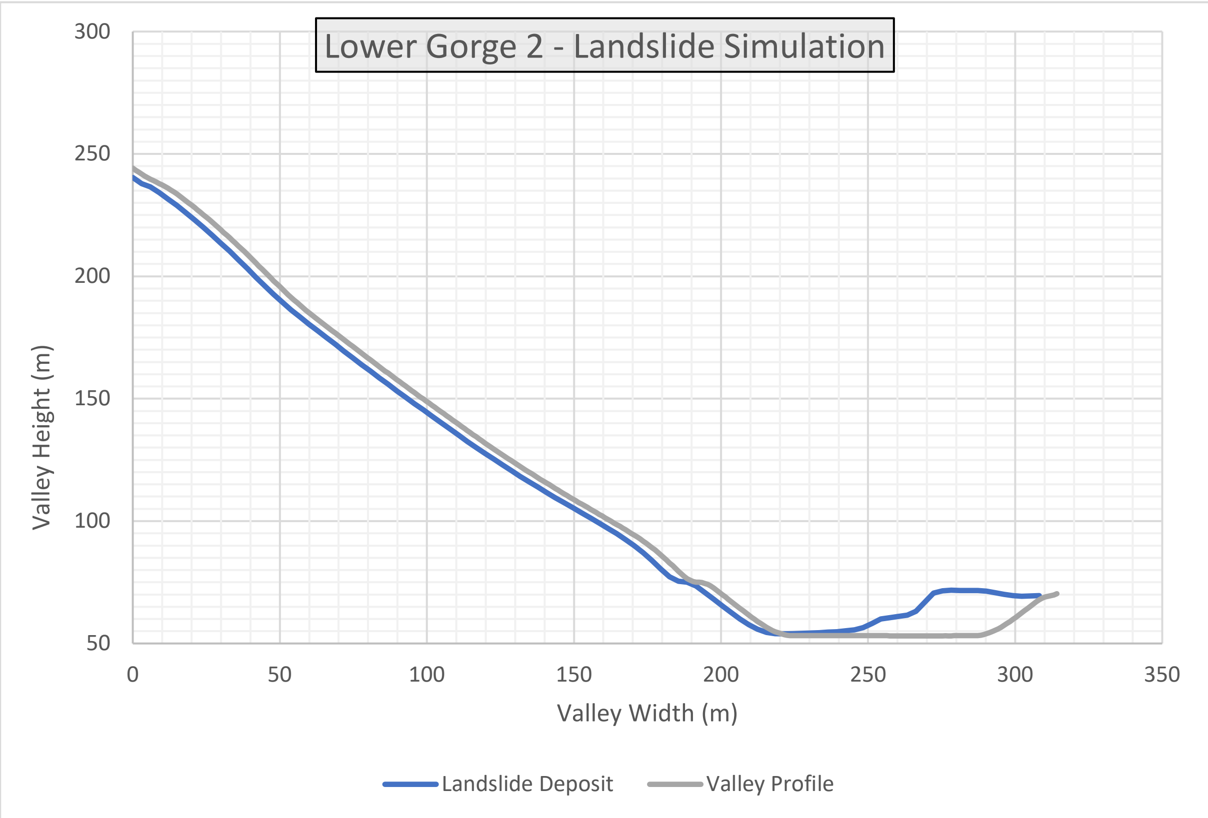

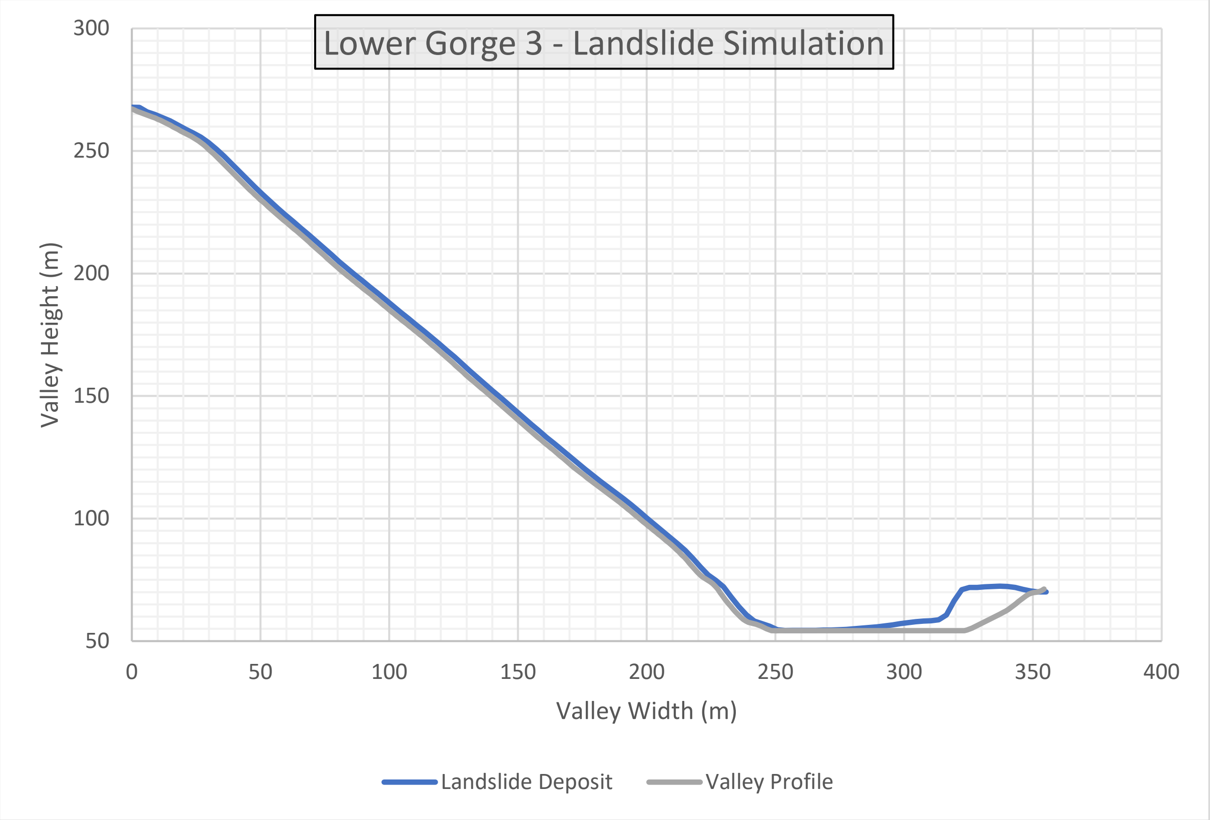
Lower Gorge 3 - Landslide Simulation
Valley Height (m)
300
250
200
150
100
50
0
50
100
150
200
250
300
350
400
Valley Width (m)
Landslide Deposit
Valley Profile

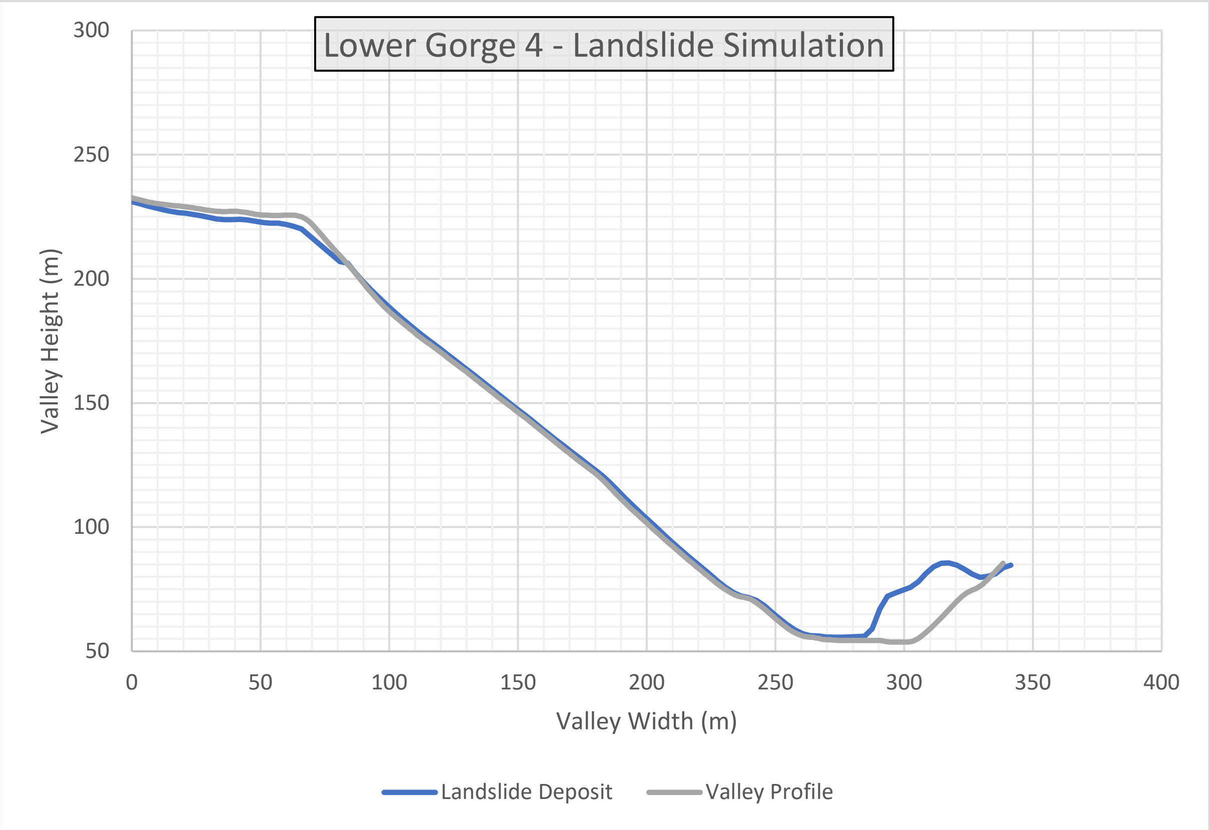
Lower Gorge 4 - Landslide Simulation
Valley Height (m)
300
250
200
150
100
50
0
50
100
150
200
250
300
350
400
Valley Width (m)
Landslide Deposit
Valley Profile

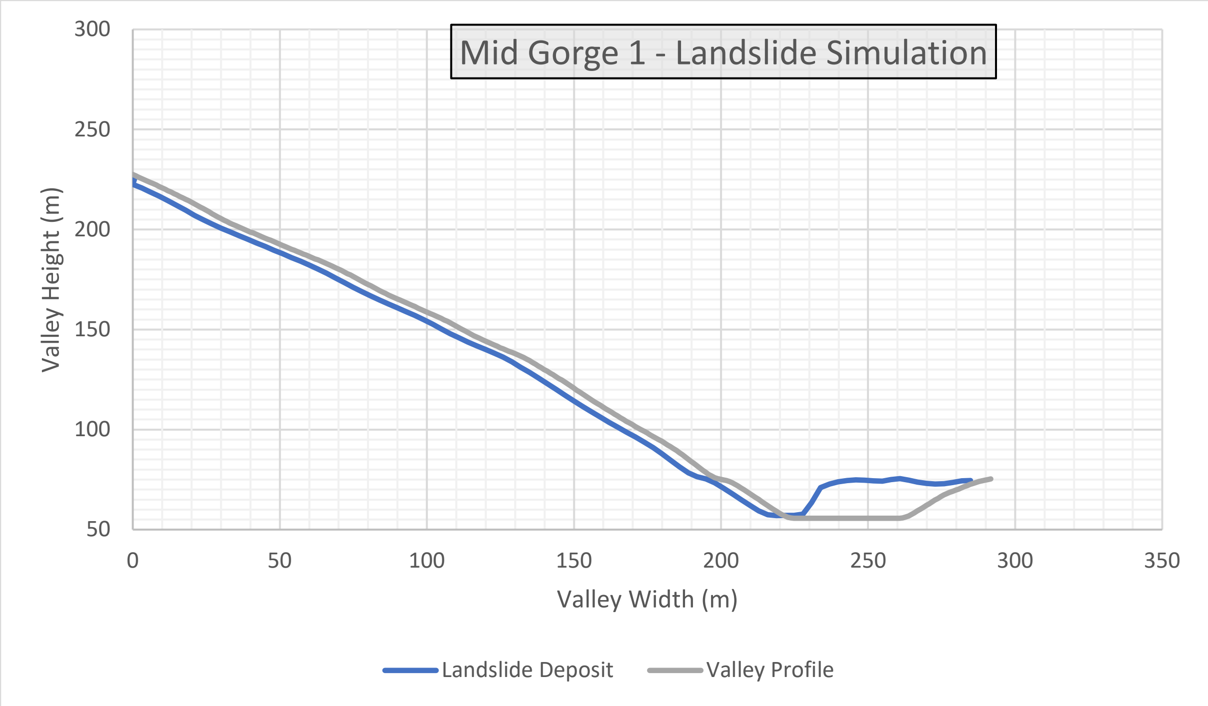
Mid Gorge 1 - Landslide Simulation
Valley Height (m)
300
250
200
150
100
50
0
50
100
150
200
250
300
350
Valley Width (m)
Landslide Deposit
Valley Profile

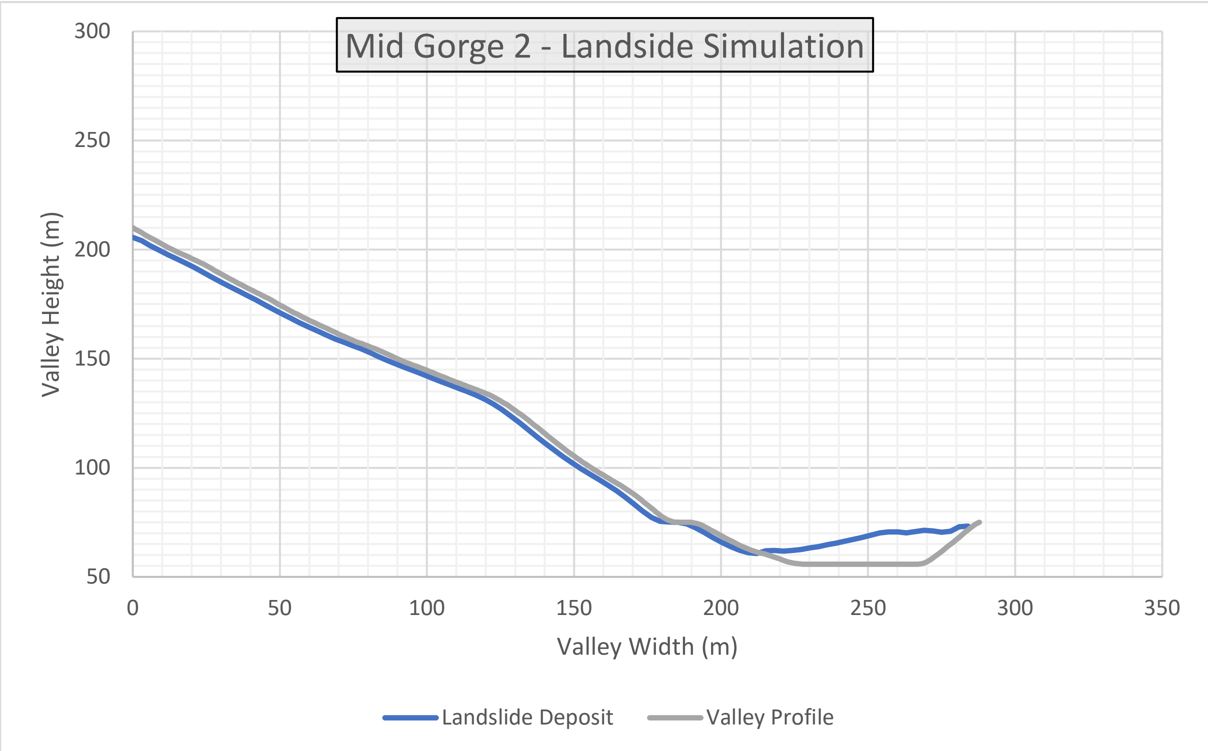
Mid Gorge 2 - Landslide Simulation
Valley Height (m)
300
250
200
150
100
50
0
50
100
150
200
250
300
350
Valley Width (m)
Landslide Deposit
Valley Profile

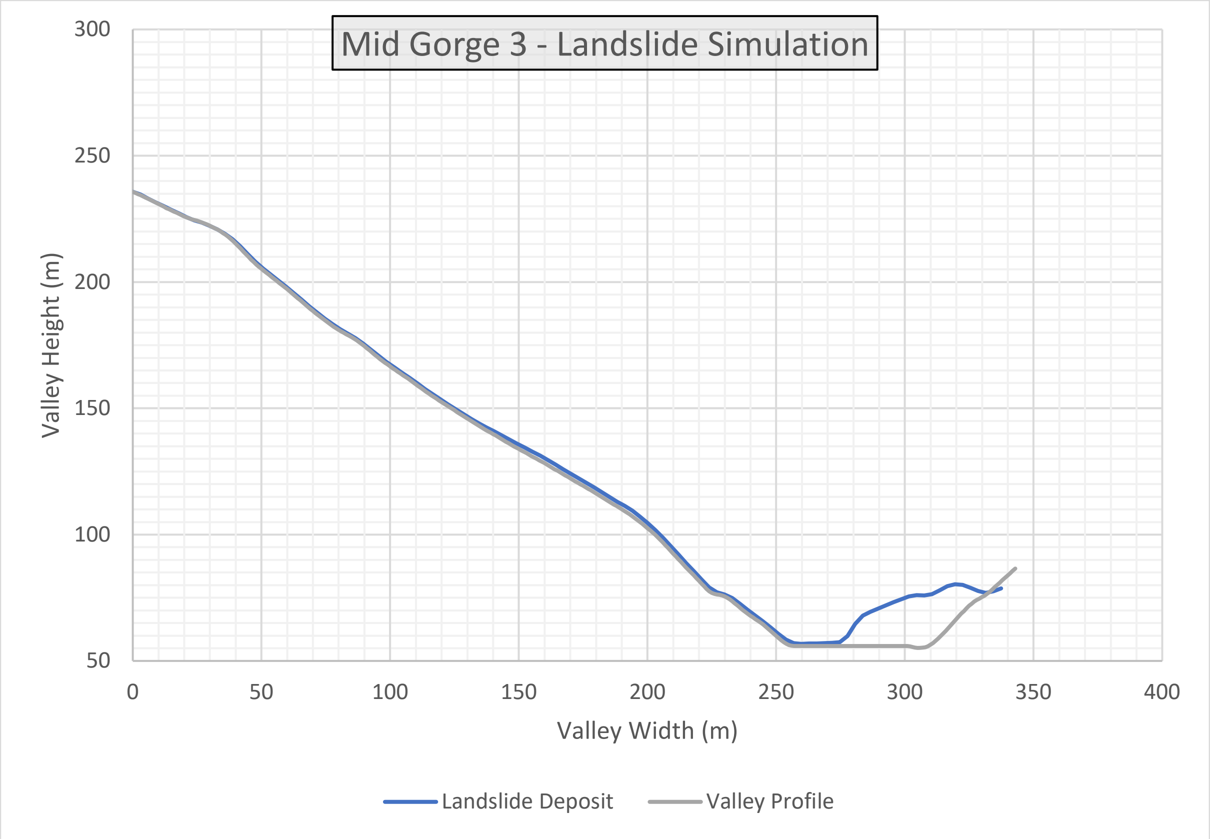
Mid Gorge 3 - Landslide Simulation
Valley Height (m)
300
250
200
150
100
50
0
50
100
150
200
250
300
350
400
Valley Width (m)
Landslide Deposit
Valley Profile

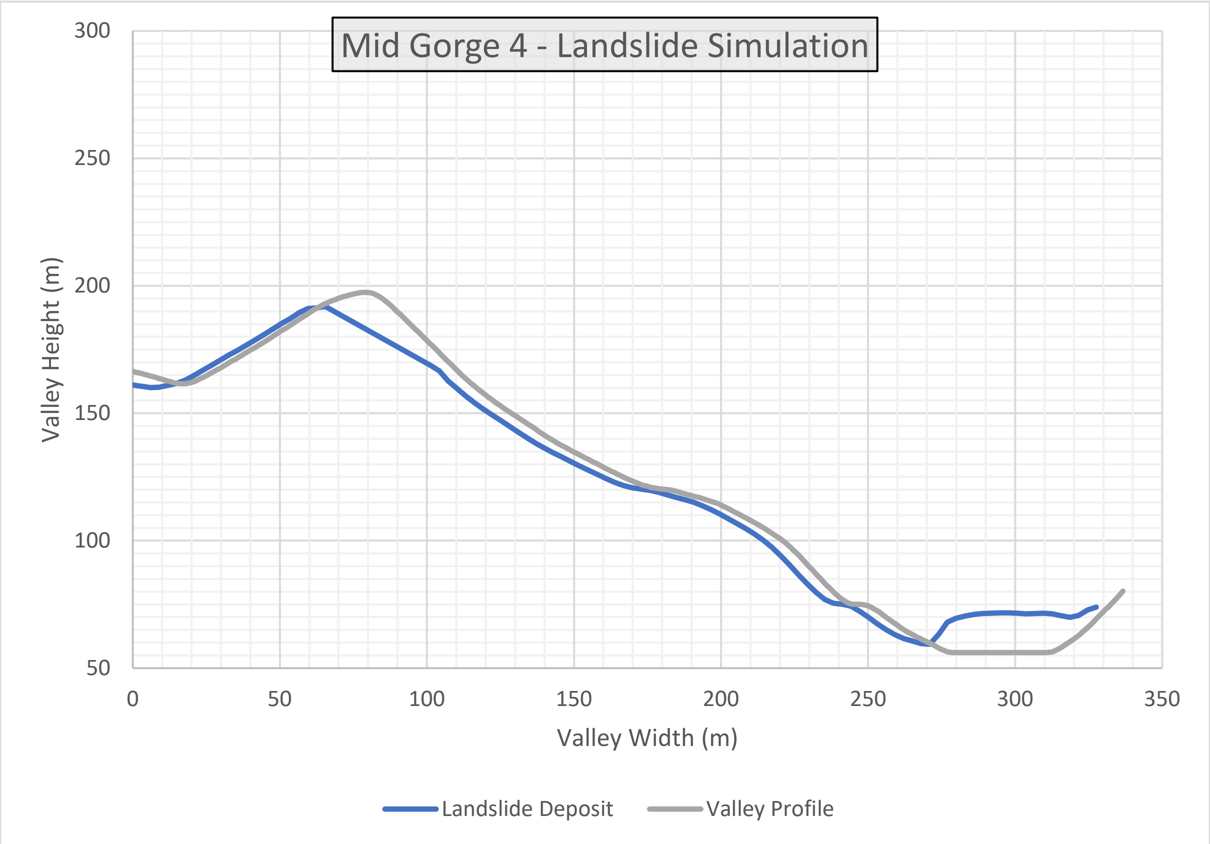
Mid Gorge 4 - Landslide Simulation
Valley Height (m)
300
250
200
150
100
50
0
50
100
150
200
250
300
350
Valley Width (m)
Landslide Deposit
Valley Profile

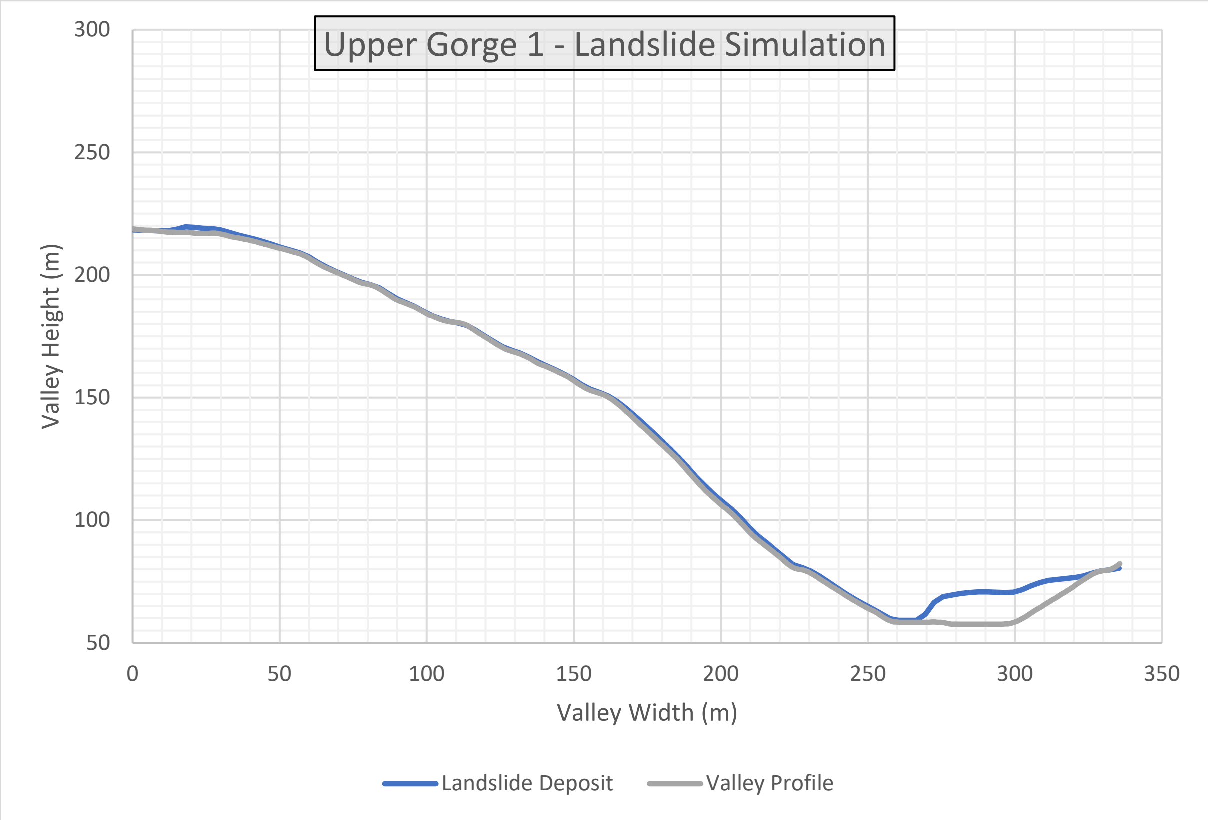
Upper Gorge 1 - Landslide Simulation
Valley Height (m)
300
250
200
150
100
50
0
50
100
150
200
250
300
350
Valley Width (m)
Landslide Deposit
Valley Profile

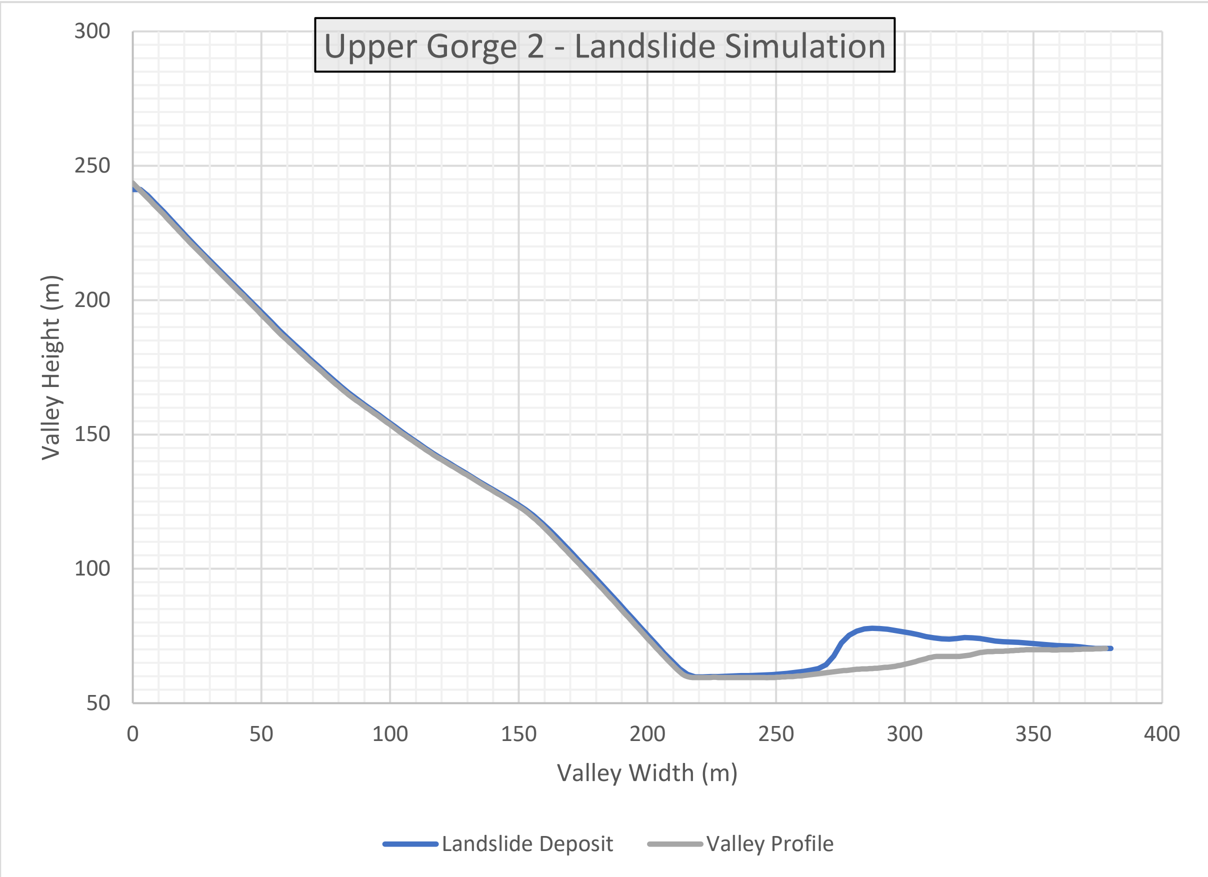
Upper Gorge 2 - Landslide Simulation
Valley Height (m)
300
250
200
150
100
50
0
50
100
150
200
250
300
350
400
Valley Width (m)
Landslide Deposit
Valley Profile

www.gns.cri.nz

Principal Location

1 Fairway Drive
Avalon
PO Box 30368
Lower Hutt
New Zealand
T +64-4-570 1444
F +64-4-570 4600

Other Locations

Dunedin Research Centre
764 Cumberland Street
Private Bag 1930
Dunedin
New Zealand
T +64-3-477 4050
F +64-3-477 5232

Wairakei Research Centre
114 Karetoto Road
Wairakei
Private Bag 2000, Taupo
New Zealand
T +64-7-374 8211
F +64-7-374 8199

National Isotope Centre
30 Gracefield Road
PO Box 31312
Lower Hutt
New Zealand
T +64-4-570 1444
F +64-4-570 4657